Accepted Manuscript

Synthesis and biological evaluation of pyrrolo[2,3-*b*]pyridine analogues as antiproliferative agents and their interaction with calf thymus DNA

Suresh Narva, Surendar Chitti, Bala Bhaskara Rao, Mallika Alvala, Nishant Jain, Kondapalli Venkata Gowri Chandra Sekhar

PII: S0223-5234(16)30149-0

DOI: 10.1016/j.ejmech.2016.02.059

Reference: EJMECH 8410

To appear in: *European Journal of Medicinal Chemistry*

Received Date: 5 November 2015

Revised Date: 23 February 2016

Accepted Date: 24 February 2016

Please cite this article as: S. Narva, S. Chitti, B.B. Rao, M. Alvala, N. Jain, K.V.G. Chandra Sekhar, Synthesis and biological evaluation of pyrrolo[2,3-*b*]pyridine analogues as antiproliferative agents and their interaction with calf thymus DNA, *European Journal of Medicinal Chemistry* (2016), doi: 10.1016/j.ejmech.2016.02.059.

Synthesis and biological evaluation of pyrrolo[2,3-b] pyridine analogues as antiproliferative agents and their interaction with calf thymus DNA

Suresh Narva[a], Surendar Chitti[a], Bala Bhaskara Rao[b], Mallika Alvala[c], Nishant Jain[b], Kondapalli Venkata Gowri Chandra Sekhar[a*] [a] *Department of Chemistry, Birla Institute of Technology and Science, Pilani, Hyderabad Campus, Hyderabad – 500 078, Telangana, India.* [b]*Centre for Chemical Biology, CSIR-Indian Institute of Chemical Technology, Tarnaka, Hyderabad-500007, Telangana, India.* [c]*National Institute of Pharmaceutical Education and Research-Hyderabad, Hyderabad-500037,Telangana, India.*

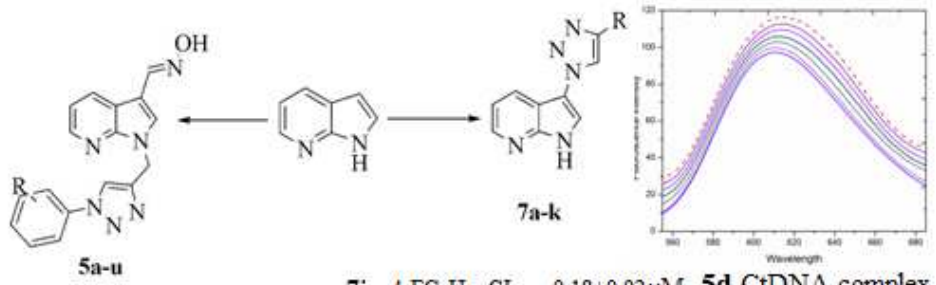

5d = 4-CF_3 = GI_{50} = 0.12±0.01 μM
5e = 4-Cl = GI_{50} = 0.13±0.01 μM
7j = 4-FC_6H_4=GI_{50} = 0.18±0.02 μM
7k = 4-$OCH_3C_6H_4$ = GI_{50} = 0.12±0.01 μM
5d-CtDNA complex

Synthesis and biological evaluation of pyrrolo[2,3-*b*]pyridine analogues as antiproliferative agents and their interaction with calf thymus DNA

Suresh Narva[a], Surendar Chitti[a], Bala Bhaskara Rao[b], Mallika Alvala[c], Nishant Jain[b], Kondapalli Venkata Gowri Chandra Sekhar[a*]

[a]*Department of Chemistry, Birla Institute of Technology and Science, Pilani, Hyderabad Campus, Jawahar Nagar, Hyderabad – 500 078, Telangana, India*

[b]*Centre for Chemical Biology, CSIR-Indian Institute of Chemical Technology, Tarnaka, Hyderabad-500007, Telangana, India*

[c]*National Institute of Pharmaceutical Education and Research-Hyderabad, Hyderabad-500037,Telangana, India*

Abstract

A series of thirty two novel pyrrolo[2,3-*b*]pyridine analogues synthesized, characterized (^{1}H NMR, ^{13}C NMR and MS) and cytotoxic evaluation of these molecules carried out over a panel of three human cancer cell lines including A549 (lung cancer), HeLa (cervical cancer) and MDA MB-231 (breast cancer), using sulforhodamine B assay method. Few molecules such as **5c**, **5d**, **5e**, **5h**, **5k**, **5m**, **5n**, **5q**, **5r**, **7f**, **7j**, **7g** and **7k** exhibited maximum growth inhibitory action against the tested cancer cell lines at lower micro molar concentration. Noticeably, compounds exhibited good growth inhibition in all three cancer cell lines in the range of 0.12 μM to 9.84μM. Further study exposed that one of the active compound **5d** could efficiently intercalate into calf thymus DNA to form **5d**-DNA complex which might block DNA replication to influence their antiproliferative activity. The molecular interactions of all the synthesized analogs were also supported by molecular docking simulations. We believe that further optimization of these compounds will lead to potential anticancer agents.

Keywords: Pyrrolo[2,3-*b*]pyridine, 1,2,3-triazole, Calf thymus DNA, Antiproliferative activity.

* Corresponding author
Tel.:+91 40 66303527 E-mail: kvgc@hyderabad.bits-pilani.ac.in; kvgcs.bits@gmail.com

1. Introduction

A systematic review of current anti-cancer literature of a variety of small heterocyclic scaffolds, such as nitrogen heterocyclic compounds, reveals an advantage of antiproliferative agents as they mimic numerous biomolecules. Among them fused heterocyclic compound such as 1*H*-pyrrolo[2,3-*b*]pyridine (7-aza-indole) is significant scaffold in medicinal chemistry. 1*H*-pyrrolo[2,3-*b*] pyridines are found in numerous natural products such as variolins, isolated from Antarctic sponge *Kirk-patrickiavarialosa* [1]. 7-aza-indoles are biologically competent organic compounds with dissimilar type of actions, such as anti-proliferative [2], protein-kinase inhibition [3], anti-inflammatory [4], antiviral [5], influenza PB2 inhibition [6], inhibition of mixed lineage kinase 3 (MLK3) [7] and selective KIT tyrosine kinase inhibition [8].

Many substituent modifications happened at different positions of 7-azindole and their biological activities were evaluated. By changing the substitutions at 3rd and 5th positions of 7-azaindole, [3,5-*d*]-7-azaindole analogues through fragment-based growing strategy [9] as phosphatidylinositol-3-kinase alpha (PI3Kα) inhibitors were developed and were found to exhibit antiangiogenic effect on cancer cells [10]. 7-azaindole containing 4-pyridyl group at the C-3 position, sulfonamide group at C-5 position analog influenced Tropomyosin-related kinase A (Trk A) binding affinity (1.67nM) and exhibited good antiproliferative activity against MCF7 cell line. This analog exhibited strong apoptotic and antiangiogenic effects by inhibiting HIF-1α and vascular endothelial growth factor (VEGF) expression and repressed the angiogenic process by inhibiting endothelial cell migration and tube formation [11].

7-azaindole containing rebeccamycin analogues have strong antiproliferative activity. They are less toxic and arrest the cell cycle in G2+M phase at 0.25 µM than rebeccamycin [12]. Cytotoxicity against various cancer cell lines is considerably enhanced by replacing the amine ligands of cisplatin by 7-azaindole analogues [13, 14]. The 7-azaindole ring scaffold plays an important role in controlling the chemical and biological properties like cellular distribution, cellular accumulation, dissimilar effects at the stage of cell cycle regulation, reduced propensity for DNA adduct repair and binding to DNA [15].

7-azaindole–chloro pyridine analogues inhibit the Cdc7 (cell division cycle 7) kinase which is necessary for activating the DNA replicative complex at the beginning of replication [16-20]. (*Z*)-2-(benzylamino)-5-(1*H*-pyrrolo[2,3-*b*]pyridin-3-ylmethylene)-1,3-thiazol-4(5*H*)-one showed 7 nM IC_{50} value and acts as a potent ATP mimetic inhibitor of Cdc7 kinase [21]. 7-azaindole core with 6-methyl substitution showed potent *in vitro* anticancer activity with enhanced metabolic stability, solubility, and oral bioavailability [22]. 6-substituted pyrrolo[2,3-*b*]pyridine-1-carboxamide analogues, new class of PARP-1 [Poly(ADP-ribose) polymerase] inhibitors, are involved in maintaining DNA integrity and in regulation of programmed cell death [23, 24] and showed potent *in vitro* and *in vivo* activity when used at a lower dose [25]. 2,5-disubstituted 7-azaindole analog, methyl 5-(2-chloro-6-methylbenzylamino)-1*H*-pyrrolo[2,3-*b*]pyridine-2-carboxylate potently inhibited Abl and Src kinases with IC_{50} values 1.4 nM and 3.4 nM respectively [26]. Hence, substituted 7-azaindoles can be well explored for the synthesis of novel anticancer agents.

It is very interesting to know that several pharmacophores like naphthofuranones, methoxyphenyl oximes, and piperazinylindenoquinolinone having oxime (hydroxylamino) as a functional group display very good anticancer activity. Tseng *et.al.*, synthesized (*Z*)-4-(hydroxyimino)naphtho[2,3-*b*]furan-9(4*H*)-one derivative which exhibited potent antiproliferative activity against selected cell lines. Oximes containing anticancer compounds are depicted in **Figure 1** [27-29].

Insert: Figure 1

1,2,3-triazoles are imperative class of heterocycles and play a major role in medicinal chemistry with antifungal [30, 31], antibacterial [32, 33], antiallergic [34], anti-inflammatory [35] and anticancer activities [36]. In recent years, copper-catalyzed azide-alkyne cycloaddition (CuAAC) reaction has become a synthetic cornerstone for conjugating building blocks with diverse functionalities [37]. Singh *et.al.*, reported 1,2,3-triazole tethered β-lactam-chalcone bifunctional hybrids as anticancer agents [38]; Duan *et.al*., synthesized 1,2,3-triazole-dithiocarbamate hybrids [39] as well as 1,2,3-triazole-dithiocarbamate-urea hybrids [40] and evaluated them for the anticancer activity against selected human tumor cell lines. Some of the compounds exhibited excellent broad spectrum anticancer activity. Ahmed *et.al*., synthesized flavone-triazole-tetrahydropyran conjugates and evaluated the compounds for anticancer activity,

in which most of the compounds exhibited IC_{50} in the range of 0.61-1.68 µM [41]. Ma *et.al.*, synthesized 1,2,3-triazole-pyrimidine hybrids, which showed IC_{50} values ranging from 1.42 to 6.52 µM against various cancer cell lines [42]. 1,2,3-triazole based anticancer agents are shown in **Figure 2**.

Insert: Figure 2.

Our newly designed scaffold consists of three prime components, i.e., 7-azaindole as a core moiety, oxime at 3rd position of 7-azaindole, and 1,2,3-triazole at 1st and 3rd position. To explore the alterations of this conserved hinge region oxime, we modified this region with 1,2,3-triazole. Herein we report the chemical synthesis of new analogues of 1*H*-pyrrolo[2,3-*b*]pyridine, that are based on some of the major chemotherapeutic pharmacophores in the area of cancer. In this study we designed and synthesized novel 7-azaindole analogues by varying substitutions at 1st and 3rd position [**scheme 1** and **scheme 2**] and evaluated them for antiproliferative activity on three different human cancer cell lines. One such derivative stood out in these screens (**Table1**) and was selected as lead molecule for CtDNA binding studies.

2. Results and discussion

2.1. *Chemistry*

The synthesis of pyrrolo[2,3-*b*]pyridine analogues **5a-u** and **7a-k** described in this study is depicted in **scheme 1** and **2**. 1*H*-pyrrolo [2,3-*b*]pyridine-3-carbaldehyde **(2)** was prepared using reported procedure of Duff reaction in the presence of hexamethylenetetramine (HMTA), acetic acid (33%) [43-45]. Formylation occurs at C-3 position of 1*H*-pyrrolo [2,3-*b*]pyridine yielding **2** in 75% yield. 1*H*-pyrrolo [2,3-*b*]pyridine-3-carbaldehyde (**2**) was treated with propargyl bromide in the presence of potassium carbonate (K_2CO_3), dimethyl formamide (DMF) to yield 1-(prop-2-ynyl)-1*H*-pyrrolo[2,3-*b*]pyridine-3-carbaldehyde **(3)**. This alkylation happened at 1st position of 1*H*-pyrrolo[2,3-*b*]pyridine-3-carbaldehyde (**2**). 1-(prop-2-ynyl)-1*H*-pyrrolo[2,3-*b*]pyridine-3-carbaldehyde oxime (**4**) was synthesized by reacting 1-(prop-2-ynyl)-1*H*-pyrrolo[2,3-*b*]pyridine-3-carbaldehyde (**3**) with hydroxylamine hydrochloride in the presence of ethanol. The title compounds (**5a-u**) were synthesized by click chemistry. 1-(prop-2-ynyl)-1*H*-pyrrolo[2,3-*b*]pyridine-3-carbaldehyde oxime (**4**) on treatement with various aromatic azides, copper sulfate pentahydrate and sodium ascorbate in aqueous DMF in one pot yielded **5a-u**. 3-bromo-1*H*-pyrrolo[2,3-*b*]pyridine **(6)** was synthesized by treating pyrrolo[2,3-*b*]pyridine with *N*-

bromosuccinimide in presence of DMF at RT [46]. 3-bromo-1*H*-pyrrolo[2,3-*b*]pyridine **(6)** was treated with various aromatic and aliphatic alkynes in the presence of sodium azide, copper sulfate pentahydrate and sodium ascorbate, L-proline, sodium carbonate in aq DMSO (9:1) to yield products **7a-k**. All the synthesized compounds were characterized and confirmed by ^{1}HNMR, ^{13}C NMR and LC-MS.

Insert: Scheme 1 and **2**

In general ^{1}H NMR of all the title compounds displayed singlet peak of *N*-1 proton (**7a-k**) in the range of 12.07-12.89 ppm. A sharp peak due to the proton of oxime OH group (**5a-u**) resonated in the range 10.73-10.80 ppm. One singlet resonated in the range of 7.18-9.01 due to the proton of triazole ring. The oxime CH protons, showed singlet in the range δ 7.92-7.97. A sharp singlet in the range 5.63-5.68 ppm corresponding to the methylene protons was observed.

2.2. *In vitro evaluation of the anticancer activity*

In vitro antiproliferative activity of the synthesized compounds **5a-u** and **7a-k** were evaluated against three types of human cancer cell lines viz; A549 (Lung cancer), HeLa (Cervical cancer) and MDA-MB-231 (Breast cancer) employing sulforhodamine B (SRB) assay method [47, 48]. For *in vitro* chemo sensitivity of tumor cell lines, numerous quick colorimetric assays are available, while MTT [3-(4,5-dimethylthiazolyl-2)-2,5 diphenyltetrazoliumbromide] assay being the most extensively used, recently the US National Cancer Institute (NCI) recommended use of the sulforhodamine B (SRB) protein stain for *in vitro* chemo sensitivity testing. The SRB assay appeared to be more responsive than MTT assay, with better linearity with cell number and higher reproducibility [49, 50]. The growth inhibition data (expressed as GI_{50}) of synthesized compounds **5a-u** and **7a-k** are shown in **Table 1**.

Insert: Table 1

From the anti-proliferative activity results, it is evident that all the synthesized compounds have comparable antiproliferative activity with GI_{50} values ranging from 0.12-9.84 μM. It is observed that, the majority of the compounds tested displayed significant growth inhibition on A549 and MDA MB 231 cancer cell lines as compared to HeLa cancer cell line. Compounds **5d** and **5k** showed potent anticancer activity against lung cancer cell line (A549) with GI_{50} values 0.12 μM and 0.16 μM and compounds **5e** and **5m** showed potency against breast cancer cell line with GI_{50}value 0.13 μM while the positive controls, doxorubicin and paclitaxel demonstrated the

GI_{50} in the range of <0.01-0.09 μM and <0.01-0.023 μM respectively. Compound **5r** is potent against breast cancer cell line with GI_{50} value 0.14 μM. Compound **7j** inhibited cell growth significantly in three human cancer cell lines with GI_{50} values 0.18μM against A549, 0.7 μM against HeLa and 0.25 μM against MDA MB 231 cell line. The compounds **7a**, **7b**, **7c**, **7d**, **7e**, **7f, 7g, 7h, 7i** and **7k** had shown comparable values against lung, cervical and breast cancer cell lines with GI_{50} values ranging from 0.17-9.84 μM as compared to the standard drugs.

Based on the results of antiproliferative activity, the structure activity relationships (SAR) for these newly synthesized compounds (**5a-u** and **7a-k**) are described as follows. It is interesting to observe that compound with electron withdrawing chloro substitution at ortho-position (**5k**) exhibits good activity (0.16 μM) against A549 cell line compared with other halo substitutions like fluoro (**5j**), bromo (**5l**) and iodo (**5m**). Compound with electron withdrawing nitro group at ortho position (**5o**) showed reduction in activity (0.95 μM) against A549 cell line. Introduction of electron withdrawing groups like trifluoromethyl (**5d**), nitro (**5h**) at para position increased the activity against A549 cell line compared to electron donating substituents like ethyl (**5a**) and methoxy (**5g**). 3, 4-di substituted compounds exhibited moderate activity against A549 cell line. 1,2,3-triazole ring at either 1st position or 3rd position on pyrrolo[2,3-*b*]pyridine did not have much effect on activity against A549 cell line. All the synthesized compounds exhibit moderate activity (0.39-1.86 μM) against HeLa cancer cell line. The compound with iodo substitution (**5m**) at ortho position showed better activity (0.13 μM) against MDA MB-231 cancer cell line compared with fluoro (**5j**), chloro (**5k**), bromo (**5l**) and nitro (**5o**) groups at ortho positions; **5e** with electron withdrawing chloro substitution at para position showed potent activity (0.13 μM) than other halo substitutions and also electron donating groups like methoxy (**5g**). 3,4-dimethoxy substitution compound showed better activity (0.14 μM) than 3,4-dimethyl, 3,4-dichloro, 3,4-difluoro compounds against MDA MB-231 cancer cell line. 1,2,3-triazole ring at 3rd position on pyrrolo[2,3-*b*]pyridine analogues from **7a-7k** showed good to moderate activity. Compound with electron withdrawing fluoro at para position (**7j**) showed good activity against all three cell lines A549, HeLa, MDA MB-231 respectively with GI_{50} of 0.18μM, 0.7μM, 0.25μM compared with electron donating substitutions at para position like methoxy (**7k**), methyl (**7b**), tertiary butyl (**7c**) and the unsubstituted one (**7a**). Based on the SAR, we note that

the halo groups like fluoro, chloro, iodo at ortho and para positions play crucial role in antiproliferative activity.

2.3. *Molecular modeling studies*

The molecular docking studies of **5a-u** and **7a-k** were performed using ALK (Human anaplastic lymphoma kinase) enzyme using Schrödinger suite 2013. Crystal co-ordinates for ALK (Human anaplastic lymphoma kinase) were taken from Protein Data Bank (PDB ID: 2XP2). Docking studies were performed using GLIDE, module of Schrödinger. Docking scores by standard precision (Glide-SP) docking were shown in **Table 1**. Molecular docking studies revealed that these compounds (**7f**, **7g** and **7i**) bind to the crizotinib binding site of the human anaplastic lymphoma kinase with a binding affinity of -8.318, -8.18 and -8.663 respectively, compared to crizotinib-8.123). The hydroxyl group of **7f**, **7g** and **7i** showed hydrogen bonding interaction with LYS 1150, ASP 1270 and GLU 1167 amino acids. This orientation is fruitful for extensive interactions such as hydrophobic interactions. Therefore, substitution with hydroxyl group in **7f**, **7g** and **7i** resulted in improved docking score, which contributed for the antiproliferative activity. Amino acid interaction pattern of active compounds **7f**, **7g** and **7i** are shown in **Figure 3** along with crizotinib (PF-02341066) as standard. Crizotinib has shown docking score of -8.123.

Insert: Figure 3

2.4. *Intercalation with Calf thymus DNA*

2.4.1. UV- Visible spectral studies

UV–visible spectroscopy is frequently used technique to discover the interaction studies between biological macromolecules and small molecules. We used UV–visible spectroscopy to investigate the absorbance spectra of **5d**-CtDNA interaction (**Figure 4**). The characteristic peak of compound **5d** alone was observed near 222nm. However, on subsequent addition of CtDNA to compound **5d**, the absorbance of compound gradually decreased, indicating hypochromic effect. Hypochromic effect interaction of compound **5d** with CtDNA indicates strong intermolecular interaction. This hypochromic effect is due to the overlap of the electron cloud of the compound **5d** with the CtDNA base pairs [51, 52]. Hypochromic effect in UV–visible spectra upon compound binding to CtDNA is a characteristic of an intercalating binding mode [53, 54].

Insert: Figure 4

The intrinsic binding constant K_b of the compound to CtDNA was determined from following equation.

$$[DNA]/|\varepsilon_a - \varepsilon_{f|} = [DNA]/|\varepsilon_b - \varepsilon_{f|} + 1/K_{b|}\, \varepsilon_b - \varepsilon_f$$

Here [DNA] represents the concentration of DNA in base pairs, and ε_a, ε_f and ε_b the apparent extinction coefficient (A_{obs}/[M]), the extinction coefficient for free complex (M), and the extinction coefficient for the free complex (M) in the fully bound form, respectively. K_b is the equilibrium binding constant (in M^{-1}) of compound binding to DNA. In plots of $[DNA]/\varepsilon_a - \varepsilon_f$ Vs [DNA], K_b is obtained by the ratio of slope to intercept (**Figure 5**). The binding constant K_b for compound **5d** is $7.16 \times 10^4\ M^{-1}$. These results indicate that the binding strength of compound **5d** is good through the intercalate mode.

Insert: Figure 5

2.4.2. Fluorescence spectral studies

The compound **5d** has no fluorescence at room temperature, so the binding of the compound with CtDNA can't be predicted directly through the emission spectra. The spectroscopic changes of Ethidium bromide (EB) on its binding to CtDNA are frequently utilized to study the interaction between CtDNA and new substances such as synthesized molecule [55, 56]. EB displays very feeble fluorescence in the aqueous solution, but in the presence of DNA it exhibits strong fluorescence because of the intercalation to the base pairs in DNA. Intensity of the EB-DNA adduct allows us to determine the affinity of the binding mode of compound **5d** for DNA. If compound can replace EB from EB-DNA, the fluorescence of the solution will be quenched as the free EB molecules are readily quenched by the adjacent water molecules [57, 58]. The fluorescence quenching of EB-CtDNA by the compound **5d** is shown in **Figure 6.** The quenching of EB-CtDNA by the compound **5d** is in good agreement with the linear Stern-Volmer equation, which provides further evidence that **5d** binds to DNA.

Insert: Figure 6

$$\frac{I_0}{I} = 1 + K_{sv}\,[Q]$$

In the above equation I_0 is the emission intensity in the absence of quencher, I is the emission intensity in the presence of quencher, K_{sv} is the Stern-Volmer quenching constant, and [Q] is the quencher concentration. The shape of Stern-Volmer plot can be used to characterize the

quenching as being predominantly dynamic or static. Plots of I_0/I versus [Q] appear to be linear. The linear relationship of I_0/I versus [Q] recommends that the quenching result for this system is a static type, means non-fluorescence complex is formed between compound **5d** and CtDNA. K_{sv} is given by the ratio of the slope to the intercept (**Figure 7)**. The K_{sv} value for the compound is 5.19×10^{-4} L M^{-1}. This data clearly indicates the interaction of **5d** with CtDNA.

Insert: Figure 7

2.5. Activation of p53 protein: Since **5d** was demonstrated to intercalate with DNA. Thus we elucidated whether 5d shows a similar mode of action in cancer cells. To achieve this, we treated HeLa cells in a dose dependent manner with **5d** at 5 and 10 μM concentrations for 24 h. p53 is a tumor suppressor protein that is activated in response to genotoxic stress. Further, we also observed potent induction of p53 protein levels in **5d** treated cells. Tubulin was used as a loading control, criztonib. Overall, our results show that **5d** elicits p53 activation in cancer cells possibly through intercalating with DNA.

Insert: Figure 8

3. Conclusion

In summary, a series of pyrrolo[2,3-*b*]pyridine analogues have been designed and synthesized, subsequent by easy reaction protocols. All the synthesized compounds were screened for their growth inhibitory activity against a panel of three different human cancer cell lines such as A549, HeLa and MDA-MB-231. Most of the tested pyrrolo[2,3-*b*]pyridine analogues displayed promising growth inhibitory activity against cancer cell lines. Among all the synthesized compounds **5c**, **5d**, **5e**, **5h**, **5k**, **5m**, **5n**, **5q**, **5r**, **7f**, **7j**, **7g** and **7k** showed maximum growth inhibitory activity against cancer cell lines at low concentrations. The specific interaction of compound **5d** with calf thymus DNA by intercalate mode, which might further block DNA replication to exert their antiproliferative activity. Our findings from this work with synthesis, antiproliferative activity, molecular modeling and DNA binding experiments demonstrate that this pyrrolo[2,3-*b*]pyridine analogues could be potential candidates for developing anticancer agents.

4. Experimental section

4.1. *Materials and Methods*

All reagents were purchased from commercial sources and used with further purification wherever necessary. 7-Azaindole was purchased from Sigma Aldrich. All reactions were monitored by analytical thin layer chromatography (TLC) performed on E-Merck 0.25 mm pre coated silica gel aluminum plates (60 F254) using mixture of pet ether and ethyl acetate. Visualization of the spots on TLC plates was achieved by exposure to UV light. Column chromatography was performed using silica gel (Acme, 100-200mesh). Solvents were dried and purified by distillation prior to use. Solvents for chromatography (Pet ether and ethyl acetate) were distilled prior to use. Evaporations were carried out under reduced pressure on Heidolph rotary evaporator. Melting points were obtained using Stuart SMP30 system and are uncorrected. ^{1}H and ^{13}C NMR spectra were recorded on Avance-III 400MHz (400 MHz for ^{1}H, 100 MHz for ^{13}C), in $CDCl_3$ or DMSO-d_6. Chemical shifts have been expressed in parts per million (δ) relative to tetramethylsilane (δ = 0.0) as an internal standard and coupling constants (*J*) in Hertz. Low-resolution mass spectra (LC-MS) were recorded on LC/MS-2020 Shimadzu. IR spectra were recorded with an FT-IR spectrophotometer (Jasco FTIR-4200). The UV-visible absorption spectroscopy was performed on a spectrometer (JASCO model V-650). The fluorescence spectral titrations were performed on a spectrofluorometer (JASCO model FP-6300).

4.2. *Chemistry*

4.2.1. Synthesis of 1H-pyrrolo [2,3-b]pyridine-3-carbaldehyde (**2**): To a solution of 1*H*-pyrrolo[2,3-*b*]pyridine (1g, 8.5mmol, 1eq) in acetic acid (33%, 15mL), hexamethylenetetramine (HMTA) (1.79g, 9.35mmol, 1.1eq) was added. The reaction mixture was refluxed at 120° C for 6h. Reaction was monitored by TLC and once complete was cooled in an ice bath. The resulting precipitate was collected and dried to afford the 1*H*-pyrrolo[2,3-*b*]pyridine-3-carbaldehyde (**2**).

4.2.1.1. Synthesis of 1-(prop-2-ynyl)-1H-pyrrolo[2,3-b]pyridine-3-carbaldehyde (**3**): To a stirred solution of 1*H*-pyrrolo[2,3-*b*]pyridine-3-carbaldehyde (0.0547 moles, 1eq) in dimethylformamide (DMF), K_2CO_3(0.1094 moles, 2eq) and propargyl bromide (0.0547 moles, 1eq) were added. Reaction mixture was stirred at ambient temperature 2h. Reaction was monitored by TLC and water was added to reaction mixture once complete and was followed by

extraction with ethyl acetate. Combined organic layers were collected and dried over anhydrous sodium sulphate. Concentrated the organic layer and purified by column chromatography with pet ether and ethyl acetate (15%) to yield **3**. Brown solid; m.p. 122-124° C; IR (KBr, cm^{-1}) 3200, 2119, 1653, 1524. ^{1}H NMR (400 MHz, $CDCl_3$) δ 10.00 (s, 1H), 8.55 (dd, *J* = 7.8, 1.6 Hz, 1H), 8.43 (dd, *J* = 4.8, 1.6 Hz, 1H), 8.13 (s, 1H), 7.30 – 7.27 (m, 1H), 5.15 (d, *J* = 2.6 Hz, 2H), 2.58 (t, *J* = 2.6 Hz, 1H). ^{13}C NMR (101 MHz, $CDCl_3$) δ 184.75, 147.84, 145.26, 137.13, 130.78, 119.28, 117.74, 116.97, 76.43, 75.22, 34.49. ESI-MS (m/z): calcd. for $C_{11}H_8N_2O$ 184.06, found 185.05 $[M + H]^+$.

4.2.1.2. Synthesis of 1-(prop-2-ynyl)-1H-pyrrolo[2,3-b]pyridine-3-carbaldehyde oxime (**4**): To a stirred ice cold solution of 1-(prop-2-ynyl)-1*H*-pyrrolo[2,3-*b*]pyridine-3-carbaldehyde (0.02173 moles, 1eq) in ethanol, hydroxylamine hydrochloride (0.0260moles, 1.2eq) was added slowly. Sodium hydroxide solution was added drop wise. Reaction mixture was stirred at room temperature for 2h and was monitored by TLC. After completion, as indicated by TLC, acetic acid was added to reaction mixture to neutralize and later filtered to get the title compound. Brown solid; m.p. 184-186° C; IR (KBr, cm^{-1}) 3480, 3237, 2124, 1626, 1572, 950. ^{1}H NMR (400 MHz, DMSO) δ 10.78 (s, 1H), 8.36 (dd, *J* = 7.8, 1.6 Hz, 1H), 8.34 (dd, *J* = 4.8, 1.6 Hz, 1H), 8.31 (s, 1H), 7.90 (s, 1H), 7.26 – 7.22 (m, 1H), 5.14 (d, *J* = 2.6 Hz, 2H), 3.42 (t, *J* = 2.6 Hz, 1H). ^{13}C NMR (101 MHz, DMSO) δ 147.31, 143.70, 130.37, 129.02, 117.30, 116.91, 108.91, 101.95, 74.49, 71.76, 33.30. ESI-MS (m/z): calcd. for $C_{11}H_9N_3O$ 199.07, found 200.05 $[M + H]^+$.

4.2.2. General procedure for the synthesis of 1-((1-substituted phenyl-1H-1,2,3-triazol-5-yl)methyl)-1H-pyrrolo[2,3-b]pyridine-3-carbaldehyde oxime (**5a-u**): To a stirred solution of compound **4** (1.0 mmol) and substituted phenyl azide (1.2 mmol) in ^{t}butanol-water (1:1) (4 mL), $CuSO_4.5H_2O$ (1 mol %) (0.2 mmol) and sodium ascorbate (5 mol %) (0.2 mmol) were added and the reaction mixture was stirred at RT for 2 h. After completion of the reaction, as indicated by TLC, butanol was removed under reduced pressure. The residue was extracted with ethyl acetate (3 x10 mL) and combined organic layers were collected and washed with saturated brine solution, dried over anhydrous $MgSO_4$ and concentrated in vacuo to get the crude product. The product was further purified by column chromatography using pet ether and ethyl acetae (40%) to afford the title compounds.

4.2.2.1. 1-((1-(4-ethylphenyl)-1H-1,2,3-triazol-4-yl)methyl)-1H-pyrrolo[2,3-b]pyridine-3-carbaldehyde oxime (**5a**). White solid; yield 65%, 0.33g, m.p. 174-176° C; IR (KBr, cm^{-1}) 3420, 3010, 1660, 1570, 950. ^{1}H NMR (400 MHz, DMSO) δ 10.79 (s, 1H), 8.77 (s, 1H), 8.37 (dd, *J* = 4.7, 1.4 Hz, 1H), 8.34 – 8.29 (m, 1H), 8.28 (s, 1H), 7.94 (s, 1H), 7.76 (d, *J* = 8.5 Hz, 2H), 7.39 (d, *J* = 8.6 Hz, 2H), 7.23 (dd, *J* = 7.8, 4.7 Hz, 1H), 5.65 (s, 2H), 2.64 (q, *J* = 7.6 Hz, 2H), 1.18 (t, *J* = 7.6 Hz, 3H). ^{13}C NMR (101 MHz, DMSO) δ 147.99, 145.00, 144.55, 144.44, 144.19, 134.89, 131.14, 130.38, 129.42, 122.19, 120.54, 117.50, 117.46, 108.74, 51.59, 28.12, 15.89. ESI-MS (m/z): calcd. for $C_{19}H_{18}N_6O$ 346.17, found 347.23 $[M + H]^+$.

4.2.2.2. 1-((1-(4-bromo-3-(trifluoromethyl)phenyl)-1H-1,2,3-triazol-4-yl)methyl)-1H-pyrrolo[2,3-b] pyridine-3-carbaldehyde oxime (**5b**). Pale yellow solid; yield 76%, 0.53g, m.p. 205-207° C; IR (KBr, cm^{-1}) 3425, 3015, 1670, 1565, 1130, 950, 575. ^{1}H NMR (400 MHz, DMSO) δ 10.79 (s, 1H), 9.01 (s, 1H), 8.36 (d, *J* = 3.8 Hz, 1H), 8.32-8.30 (m, 2H), 8.28 (s, 1H), 8.14 (dd, *J* = 8.7, 2.0 Hz, 1H), 8.08 (d, *J* = 8.7 Hz, 1H), 7.94 (s, 1H), 7.23 (dd, *J* = 7.8, 4.7 Hz, 1H), 5.67 (s, 2H). ^{13}C NMR (101 MHz, DMSO) δ 147.97, 145.20, 144.37, 144.22, 137.07, 136.34, 131.16, 130.46, 125.70, 122.70, 121.48, 120.06, 120.00, 118.98, 117.53, 117.46, 108.81, 51.61. ESI-MS (m/z): calcd. for $C_{18}H_{12}BrF_3N_6O$ 464.02, found 465.09 $[M + H]^+$.

4.2.2.3. 1-((1-(4-bromophenyl)-1H-1,2,3-triazol-4-yl)methyl)-1H-pyrrolo[2,3-b]pyridine-3-carbaldehyde oxime (**5c**). Pale yellow solid; yield 84%, 0.5g, m.p. 166-168° C; IR (KBr, cm^{-1}) 3462, 3012, 1658, 1568, 953, 595. ^{1}H NMR (400 MHz, $CDCl_3$) δ 10.79 (s, 1H), 8.76 (s, 1H), 8.36 (dd, *J* = 4.7, 1.4 Hz, 1H), 8.32 – 8.29 (m, 1H), 8.28 (s, 1H), 7.94 (s, 1H), 7.78 (d, *J* = 8.5 Hz, 2H), 7.41 (d, *J* = 8.6 Hz, 2H), 7.25 (dd, *J* = 7.8, 4.7 Hz, 1H), 5.66 (s, 2H). ^{13}C NMR (100.61 MHz, $CDCl_3$) δ 147.95, 145.03, 144.56, 144.43, 144.15, 134.86, 131.12, 130.36, 129.48, 122.12, 120.58, 117.50, 117.46, 108.75, 51.49. ESI-MS (m/z): calcd. for $C_{17}H_{13}BrN_6O$ 396.03, found 397.11 $[M + H]^+$.

4.2.2.4. 1-((1-(4-(trifluoromethyl)phenyl)-1H-1,2,3-triazol-4-yl)methyl)-1H-pyrrolo[2,3-b]pyridine-3-carbaldehyde oxime (**5d**). Pale yellow solid; yield 86%, 0.5g, m.p. 178-179° C; IR (KBr, cm^{-1}) 3435, 3008, 1648, 1572, 1125, 952. ^{1}H NMR (400 MHz, $CDCl_3$) δ 10.75 (s, 1H),

8.95 (s, 1H), 8.36 (dd, *J* = 4.7, 1.4 Hz, 1H), 8.32 – 8.29 (m, 1H), 8.28 (s, 1H), 8.13 (d, *J* = 8.5 Hz, 2H), 7.97 (d, *J* = 8.6 Hz, 2H),7.94 (s, 1H), 7.24 (dd, *J* = 7.8, 4.7 Hz, 1H), 5.67 (s, 2H). ^{13}C NMR (100.61 MHz, $CDCl_3$) δ 147.95, 145.03, 144.56, 144.43, 144.15, 134.86, 131.12, 130.36, 129.48, 122.12, 121.34, 120.58, 117.50, 117.46, 108.75, 51.48. ESI-MS (m/z): calcd. for $C_{18}H_{13}F_3N_6O$ 386.11, found 387.19 $[M + H]^+$.

4.2.2.5. 1-((1-(4-chlorophenyl)-1H-1,2,3-triazol-4-yl)methyl)-1H-pyrrolo[2,3-b]pyridine-3-carbaldehyde oxime (**5e**). Pale yellow solid; yield 76%, 0.4g, m.p. 173-175° C; IR (KBr, cm^{-1}) 3398, 3012, 1652, 1574, 956, 792.^{1}H NMR (400 MHz, DMSO) δ 10.78 (s, 1H), 8.78 (s, 1H), 8.38 (dd, *J* = 4.7, 1.4 Hz, 1H), 8.34 – 8.29 (m, 1H), 8.28 (s, 1H), 7.93 (s, 1H), 7.77 (d, *J* = 8.5 Hz, 2H), 7.38 (d, *J* = 8.6 Hz, 2H), 7.26 (dd, *J* = 7.8, 4.7 Hz, 1H), 5.65 (s, 2H). ^{13}C NMR (101 MHz, DMSO) δ 147.98, 145.02, 144.54, 144.43, 144.17, 134.88, 131.15, 130.37, 129.45, 122.17, 120.54, 117.50, 117.46, 108.74, 51.56. ESI-MS (m/z): calcd. for $C_{17}H_{13}ClN_6O$ 352.08, found 353.16 $[M + H]^+$.

4.2.2.6. 1-((1-(4-fluorophenyl)-1H-1,2,3-triazol-4-yl)methyl)-1H-pyrrolo[2,3-b]pyridine-3-carbaldehyde oxime (**5f**). Pale yellow solid; yield 79%, 0.4g, m.p. 116-118° C; IR (KBr, cm^{-1}) 3430, 3010, 1635, 1565, 1235, 945. ^{1}H NMR (400 MHz, DMSO) δ 10.79 (s, 1H), 8.81 (s, 1H), 8.37 (dd, *J* = 4.7, 1.4 Hz, 1H), 8.33 – 8.29 (m, 1H), 8.28 (s, 1H), 7.92 (s, 1H), 7.78 (d, *J* = 8.5 Hz, 2H), 7.36 (d, *J* = 8.6 Hz, 2H), 7.28 (dd, *J* = 7.8, 4.7 Hz, 1H), 5.67 (s, 2H). ^{13}C NMR (101 MHz, DMSO) δ 147.98, 145.08, 144.52, 144.42, 144.19, 134.87, 131.16, 130.34, 129.46, 122.18, 120.53, 117.51, 117.46, 108.74, 51.56. ESI-MS (m/z): calcd. for $C_{17}H_{13}FN_6O$ 336.11, found 337.19 $[M + H]^+$.

4.2.2.7. 1-((1-(4-methoxyphenyl)-1H-1,2,3-triazol-4-yl)methyl)-1H-pyrrolo[2,3-b] pyridine-3-carbaldehyde oxime (**5g**). Brown solid; yield 68%, 0.35g, m.p. 172-173° C; IR (KBr, cm^{-1}) 3420, 3005, 1665, 1575, 1210, 960. ^{1}H NMR (400 MHz, DMSO) δ 10.73 (s, 1H), 8.69 (s, 1H), 8.37 (dd, *J* = 4.7, 1.4 Hz, 1H), 8.33 – 8.28 (m, 1H), 8.26 (s, 1H), 7.92 (s, 1H), 7.78 (d, *J* = 8.5 Hz, 2H), 7.28 (dd, *J* = 7.8, 4.7 Hz, 1H), 7.16 (d, *J* = 8.6 Hz, 2H), 5.63 (s, 2H), 3.81 (s, 3H). ^{13}C NMR (101 MHz, DMSO) δ 147.96, 145.04, 144.54, 144.46, 144.18, 134.86, 131.17, 130.36,

129.46, 122.18, 120.53, 117.51, 117.46, 108.74, 57.45, 51.56. ESI-MS (m/z): calcd. for $C_{18}H_{16}N_6O_2$ 348.13, found 349.21 $[M + H]^+$.

4.2.2.8. 1-((1-(4-nitrophenyl)-1H-1,2,3-triazol-4-yl)methyl)-1H-pyrrolo[2,3-b]pyridine-3-carbaldehyde oxime (**5h**). Yellow solid; yield 90%, 0.49g, m.p. 199-201° C; IR (KBr, cm^{-1}) 3440, 3002, 1645, 1565, 1520, 1340, 950. ^{1}H NMR (400 MHz, DMSO) δ 10.76 (s, 1H), 8.76 (s, 1H), 8.36 (dd, *J* = 4.7, 1.4 Hz, 1H), 8.34 – 8.28 (m, 1H), 8.27 (s, 1H), 7.94 (s, 1H), 7.78 (d, *J* = 8.5 Hz, 2H), 7.39 (d, *J* = 8.6 Hz, 2H), 7.27 (dd, *J* = 7.8, 4.7 Hz, 1H), 5.66 (s, 2H). ^{13}C NMR (101 MHz, DMSO) δ 147.96, 145.06, 144.53, 144.44, 144.16, 134.83, 131.16, 130.38, 129.45, 122.17, 120.54, 117.50, 117.46, 108.74, 51.58. ESI-MS (m/z): calcd. for $C_{17}H_{13}N_7O_3$ 363.11, found 364.18 $[M + H]^+$.

4.2.2.9. 1-((1-(4-iodophenyl)-1H-1,2,3-triazol-4-yl)methyl)-1H-pyrrolo[2,3-b]pyridine-3-carbaldehyde oxime (**5i**). Brown solid; yield 87%, 0.58g, m.p. 180-182° C; IR (KBr, cm^{-1}) 3436, 3009, 1643, 1574, 951, 520. ^{1}H NMR (400 MHz, DMSO) δ 10.77 (s, 1H), 8.76 (s, 1H), 8.38 (dd, *J* = 4.7, 1.4 Hz, 1H), 8.34 – 8.29 (m, 1H), 8.28 (s, 1H), 7.93 (s, 1H), 7.78 (d, *J* = 8.5 Hz, 2H), 7.36 (d, *J* = 8.6 Hz, 2H), 7.26 (dd, *J* = 7.8, 4.7 Hz, 1H), 5.67 (s, 2H). ^{13}C NMR (101 MHz, DMSO) δ 147.93, 145.11, 144.58, 144.42, 144.18, 134.83, 131.16, 130.38, 129.45, 122.17, 120.54, 117.51, 117.46, 108.72, 51.56. ESI-MS (m/z): calcd. for $C_{17}H_{13}IN_6O$ 444.02, found 445.11 $[M + H]^+$.

4.2.2.10. 1-((1-(2-fluorophenyl)-1H-1,2,3-triazol-4-yl)methyl)-1H-pyrrolo[2,3-b]pyridine-3-carbaldehyde oxime (**5j**). Pale yellow solid; yield 87%, 0.58g, m.p. 165-166° C; IR (KBr, cm^{-1}) 3423, 3005, 1639, 1585, 1310, 945. ^{1}H NMR (400 MHz, DMSO) δ 10.80 (s, 1H), 8.60 (s, 1H), 8.38 (dd, *J* = 4.7, 1.4 Hz, 1H), 8.32-8.30(m, 2H), 7.97 (s, 1H), 7.76 (dd, *J* = 7.75 Hz, 1H), 7.68 (dd, *J* = 7.67 Hz, 1H), 7.61 (td, *J* = 7.7, 1.8 Hz, 1H), 7.55 (td, *J* = 7.6, 1.5 Hz, 1H). 7.24 (dd, *J* = 7.24 Hz, 1H), 5.68 (s, 2H). ^{13}C NMR (100.61 MHz, $CDCl_3$) δ 148.21, 147.32, 142.25, 135.32, 133.82, 132.86, 132.02, 131.27, 130.16, 129.03, 128.87, 126.34, 119.73, 119.04, 118.51, 101.17, 52.72. ESI-MS (m/z): calcd. for $C_{17}H_{13}FN_6O$ 336.11, found 337.17 $[M + H]^+$.

4.2.2.11. 1-((1-(2-chlorophenyl)-1H-1,2,3-triazol-4-yl)methyl)-1H-pyrrolo[2,3-b]pyridine-3-carbaldehyde oxime (**5k**). Brown solid; yield 76%, 0.4g, m.p. 168-169° C; IR (KBr, cm^{-1})

3395, 3002, 1676, 1581, 955, 810. ^{1}H NMR (400 MHz, DMSO) δ 10.80 (s, 1H), 8.60 (s, 1H), 8.38 (dd, *J* = 4.7, 1.4 Hz, 1H), 8.32-8.30(m, 2H), 7.97 (s, 1H), 7.76 (dd, *J* = 7.75 Hz, 1H), 7.68 (dd, *J* = 7.67 Hz, 1H), 7.61 (td, *J* = 7.7, 1.8 Hz, 1H), 7.55 (td, *J* = 7.6, 1.5 Hz, 1H). 7.24 (dd, *J* = 7.24 Hz, 1H), 5.68 (s, 2H). ^{13}C NMR (100.61 MHz, $CDCl_3$) δ 148.00, 144.44, 144.22, 143.63, 134.84, 132.13, 131.18, 130.98, 130.45, 130.13, 128.91, 128.86, 126.25, 117.52, 117.44, 108.70, 51.33. ESI-MS (m/z): calcd. for $C_{17}H_{13}ClN_6O$ 352.08, found 353.17 $[M + H]^+$.

4.2.2.12. 1-((1-(2-bromophenyl)-1H-1,2,3-triazol-4-yl)methyl)-1H-pyrrolo[2,3-b]pyridine-3-carbaldehyde oxime (**5l**). Brown solid; yield 87%, 0.51g, m.p. 152-154° C; IR (KBr, cm^{-1}) 3467, 3043, 1665, 1586, 943, 628. ^{1}H NMR (400 MHz, DMSO) δ 10.78 (s, 1H), 8.56 (s, 1H), 8.38 (dd, *J* = 4.7, 1.4 Hz, 1H), 8.32-8.30(m, 2H), 7.97 (s, 1H), 7.76 (dd, *J* = 7.75 Hz, 1H), 7.68 (dd, *J* = 7.67 Hz, 1H), 7.61 (td, *J* = 7.7, 1.8 Hz, 1H), 7.55 (td, *J* = 7.6, 1.5 Hz, 1H). 7.24 (dd, *J* = 7.24 Hz, 1H), 5.66 (s, 2H). ^{13}C NMR (100.61 MHz, $CDCl_3$) δ 148.00, 144.44, 144.22, 143.63, 134.84, 132.13, 131.18, 130.98, 130.45, 130.13, 128.91, 128.86, 126.25, 117.52, 117.44, 108.70, 51.33. ESI-MS (m/z): calcd. for $C_{17}H_{13}BrN_6O$ 396.03, found 397.12 $[M + H]^+$.

4.2.2.13. 1-((1-(2-iodophenyl)-1H-1,2,3-triazol-4-yl)methyl)-1H-pyrrolo[2,3-b]pyridine-3-carbaldehyde oxime (**5m**). Pale yellow; yield 78%, 0.52g, m.p.154-156° C; IR (KBr, cm^{-1}) 3395, 3024, 1654, 1589, 950, 557. ^{1}H NMR (400 MHz, DMSO) δ 10.79 (s, 1H), 8.56 (s, 1H), 8.36 (dd, *J* = 4.7, 1.4 Hz, 1H), 8.32-8.29 (m, 2H), 7.97 (s, 1H), 7.76 (dd, *J* = 7.75 Hz, 1H,), 7.68 (dd, *J* = 7.67 Hz, 1H), 7.61 (td, *J* = 7.7, 1.8 Hz, 1H), 7.55 (td, *J* = 7.6, 1.5 Hz, 1H). 7.24 (dd, *J* = 7.24 Hz, 1H), 5.68 (s, 2H). ^{13}C NMR (100.61 MHz, $CDCl_3$) δ 148.00, 144.44, 144.22, 143.63, 134.84, 132.13, 131.18, 130.98, 130.45, 130.13, 128.91, 128.86, 126.25, 117.52, 117.44, 108.70, 51.28. ESI-MS (m/z): calcd. for $C_{17}H_{13}IN_6O$ 444.02, found 445.11 $[M + H]^+$.

4.2.2.14. 1-((1-(3-methoxyphenyl)-1H-1,2,3-triazol-4-yl)methyl)-1H-pyrrolo[2,3-b] pyridine-3-carbaldehyde oxime (**5n**). Brown solid; yield 91%, 0.47g, m.p. 148-150° C; IR (KBr, cm^{-1}) 3425, 3032, 1658, 1570, 1235, 945. ^{1}H NMR (400 MHz, DMSO) δ 10.78 (s, 1H), 8.58 (s, 1H), 8.38 (dd, *J* = 4.7, 1.4 Hz, 1H), 8.32-8.28 (m, 2H), 7.96 (s, 1H), 7.76 (s, 1H), 7.71 (s,1H), 7.68 (d, *J* = 7.25 Hz, 1H), 7.66 (t, *J* = 7.7 Hz, 1H), 7.24 (d, *J* = 7.24 Hz, 1H), 5.65 (s, 2H), 3.81 (s, 3H). ^{13}C NMR (101 MHz, DMSO) 148.12, 144.43, 144.21, 143.62, 134.81, 132.72, 131.34,

130.21, 130.62, 130.11, 128.91, 128.12, 126.25, 117.52, 117.44, 108.72, 56.23, 51.28. ESI-MS (m/z): calcd. for $C_{18}H_{16}N_6O_2$ 348.13, found 349.19 $[M + H]^+$.

4.2.2.15. 1-((1-(2-nitrophenyl)-1H-1,2,3-triazol-4-yl)methyl)-1H-pyrrolo[2,3-b]pyridine-3-carbaldehyde oxime (**5o**). Yellow solid; yield 67%, 0.36g, m.p. 189-190° C; IR (KBr, cm^{-1}) 3420, 3081, 1685, 1580, 1512, 1325, 940. ^{1}H NMR (400 MHz, DMSO) δ 10.75 (s, 1H), 8.69 (s, 1H), 8.37 (dd, *J* = 4.7, 1.4 Hz, 1H), 8.32-8.29 (m, 1H), 8.28 (s,1H), 8.21 (d, 1H), 7.93 (s, 1H), 7.90 (d, *J* = 7.75 Hz, 1H), 7.82 (dd, *J* = 7.6, 1.5 Hz, 2H), 7.24 (dd, *J* = 7.24,1.4 Hz, 1H), 5.67 (s, 2H). ^{13}C NMR (101 MHz, DMSO) δ 147.99, 144.39, 144.25, 138.01, 134.82, 131.65, 131.14, 130.46, 129.44, 128.07, 125.96, 125.39, 119.20, 117.54, 117.44, 108.78, 51.60. ESI-MS (m/z): calcd. for $C_{17}H_{13}N_7O_3$ 363.11, found 364.19 $[M + H]^+$.

4.2.2.16. 1-((1-(3-chloro-4-fluorophenyl)-1H-1,2,3-triazol-4-yl)methyl)-1H-pyrrolo[2,3-b]pyridine-3-carbaldehyde oxime (**5p**). Brown solid; yield 87%, 0.48g, m.p. 186-188° C; IR (KBr, cm^{-1}) 3467, 3015, 1651, 1578, 1125, 958, 814. ^{1}H NMR (400 MHz, DMSO) δ 10.79 (s, 1H), 8.83 (s, 1H), 8.36 (dd, *J* = 4.7, 1.6 Hz, 1H), 8.30 (dd, *J* = 7.8, 1.6 Hz, 1H), 8.28 (s, 1H), 8.18 (dd, *J* = 6.4, 2.7 Hz, 1H), 7.95 – 7.91 (m, 2H) 7.63 (t *J* = 6.0 Hz, 1H), 7.23 (dd, *J* = 7.8, 4.7 Hz, 1H), 5.66 (s, 2H). ^{13}C NMR (101 MHz, DMSO) δ 147.98, 144.98, 144.39, 144.22, 133.95, 131.18, 130.46, 122.83, 122.62, 121.39, 121.08, 118.63, 118.40, 117.52, 117.45, 108.78, 51.62. ESI-MS (m/z): calcd. for $C_{17}H_{12}ClFN_6O$ 370.07, found 371.13 $[M + H]^+$.

4.2.2.17. 1-((1-(3,4-dichlorophenyl)-1H-1,2,3-triazol-4-yl)methyl)-1H-pyrrolo[2,3-b]pyridine-3-carbaldehyde oxime (**5q**). Pale yellow solid; yield 81%, 0.47g, m.p. 178-180° C; IR (KBr, cm^{-1}) 3410, 3080, 1660, 1590, 960, 825. ^{1}H NMR (400 MHz, DMSO) δ 10.76 (s, 1H), 8.81 (s, 1H), 8.38 (dd, *J* = 4.7, 1.6 Hz, 1H), 8.31 (dd, *J* = 7.8, 1.6 Hz, 1H), 8.26 (s, 1H), 8.18 (dd, *J* = 6.4, 2.7 Hz, 1H), 7.95 – 7.91 (m, 2H) 7.62 (t,*J* = 6.0 Hz, 1H), 7.21 (dd, *J* = 7.8, 4.7 Hz, 1H), 5.64 (s, 2H). ^{13}C NMR (101 MHz, DMSO) δ 148.12, 144.91, 144.32, 144.22, 133.94, 131.12, 130.65, 122.75, 122.21, 121.39, 121.08, 118.63, 118.40, 117.52, 117.15, 108.72, 51.64. ESI-MS (m/z): calcd. for $C_{17}H_{12}Cl_2N_6O$ 386.04, found 387.12 $[M + H]^+$.

4.2.2.18. 1-((1-(3,4-difluorophenyl)-1H-1,2,3-triazol-4-yl)methyl)-1H-pyrrolo[2,3-b]pyridine-3-carbaldehyde oxime (**5r**). White solid; yield 72%, 0.38g, m.p. 168-169° C; IR (KBr, cm^{-1}) 3395, 3029, 1651, 1583, 1280, 954. ^{1}H NMR (400 MHz, DMSO) δ 10.78 (s, 1H), 8.84 (s, 1H), 8.36 (dd, *J* = 4.7, 1.6 Hz, 1H), 8.30 (dd, *J* = 7.8, 1.6 Hz, 1H), 8.27 (s, 1H), 8.19 (dd, *J* = 6.4, 2.7 Hz, 1H), 7.95 – 7.91 (m, 2H) 7.62 (t,*J* = 6.0 Hz, 1H), 7.23 (dd, *J* = 7.8, 4.7 Hz, 1H), 5.65 (s, 2H). ^{13}C NMR (101 MHz, DMSO) δ 148.14, 144.92, 144.32, 144.22, 133.94, 131.12, 130.65, 122.75, 122.21, 121.41, 121.08, 118.63, 118.40, 117.54, 117.16, 108.74, 51.68. ESI-MS (m/z): calcd. for $C_{17}H_{12}F_2N_6O$ 354.11, found 355.19 $[M + H]^+$.

4.2.2.19. 1-((1-(3,4-dimethoxyphenyl)-1H-1,2,3-triazol-4-yl)methyl)-1H-pyrrolo[2,3-b]pyridine-3-carbaldehyde oxime (**5s**). Brown solid; yield 86%, 0.49g, m.p. 152-153° C; IR (KBr, cm^{-1}) 3410, 3020, 1650, 1580, 1170, 945. ^{1}H NMR (400 MHz, DMSO) δ 10.74 (s, 1H), 8.71 (s, 1H), 8.37 (dd, *J* = 4.7, 1.6 Hz, 1H), 8.35 – 8.29 (m, 1H), 8.27 (s,1H), 7.93 (s, 1H), 7.66 (d, *J* = 2.0 Hz, 1H), 7.56 (dd, *J* = 8.1, 2.3 Hz, 1H), 7.29 (d, *J* = 8.2 Hz, 1H), 7.23 (dd, *J* = 7.8, 4.7 Hz, 1H), 5.63 (s, 2H), 3.29 (s, 3H), 3.26 (s, 3H). ^{13}C NMR (100.61 MHz, $CDCl_3$) δ 149.69, 149.32, 147.98, 144.43, 144.37, 144.20, 131.17, 130.46, 130.38, 122.37, 117.51, 117.44, 112.66, 112.35, 108.72, 105.09, 56.31, 56.22, 51.61. ESI-MS (m/z): calcd. for $C_{19}H_{18}N_6O_3$ 378.14, found 379.22 $[M + H]^+$.

4.2.2.20. 1-((1-(3,4-dimethylphenyl)-1H-1,2,3-triazol-4-yl)methyl)-1H-pyrrolo[2,3-b] pyridine-3-carbaldehyde oxime (**5t**). Brown solid; yield 75%, 0.39g, m.p. 188-190° C; IR (KBr, cm^{-1}) 3420, 3038, 1657, 1579, 943. ^{1}H NMR (400 MHz, DMSO) δ 10.79 (s, 1H), 8.72 (s, 1H), 8.37 (dd, *J* = 4.7, 1.6 Hz, 1H), 8.32 – 8.30 (m, 1H), 8.28 (s,1H), 7.94 (s, 1H), 7.66 (d, *J* = 2.0 Hz, 1H), 7.56 (dd, *J* = 8.1, 2.3 Hz, 1H), 7.29 (d, *J* = 8.2 Hz, 1H), 7.23 (dd, *J* = 7.8, 4.7 Hz, 1H), 5.64 (s, 2H), 2.27 (s, 3H), 2.25 (s, 3H). ^{13}C NMR (101 MHz, DMSO) δ 147.98, 144.53, 144.44, 144.20, 138.54, 137.52, 134.88, 131.20, 130.95, 130.45, 122.03, 121.30, 117.72, 117.50, 117.45, 108.74, 51.61, 19.83, 19.41. ESI-MS (m/z): calcd. for $C_{19}H_{18}N_6O$ 346.15, found 347.23 $[M + H]^+$.

4.2.2.21. 1-((1-(benzo[d][1,3]dioxol-5-yl)-1H-1,2,3-triazol-4-yl)methyl)-1H-pyrrolo[2,3-b]pyridine-3-carbaldehyde oxime (**5u**). Brown solid; yield 88%, 0.48g, m.p. 208-210° C; IR

(KBr, cm^{-1}) 3398 3029, 1654, 1586, 1210, 956. ^{1}H NMR (400 MHz, DMSO) δ 10.78 (s, 1H), 8.82 (s, 1H), 8.38 (dd, *J* = 4.7, 1.6 Hz, 1H), 8.31 (dd, *J* = 7.8, 1.6 Hz, 1H), 8.26 (s, 1H), 8.18 (dd, *J* = 6.4, 2.7 Hz, 1H), 7.95 – 7.91 (m, 2H) 7.62 (t *J* = 6.0 Hz, 1H), 7.21 (dd, *J* = 7.8, 4.7 Hz, 1H), 5.67 (s, 2H), 3.91 (s, 2H). ^{13}C NMR (101 MHz, DMSO) δ 148.65, 144.91, 144.37,144.22, 133.99, 131.12, 130.63, 122.75, 122.21, 121.39, 121.08, 118.66, 118.40, 117.52, 117.16, 108.72, 58.23, 51.66. ESI-MS (m/z): calcd. for $C_{18}H_{14}N_6O_3$362.11, found 363.21 $[M + H]^+$.

4.2.2.22.

4.2.3. Synthesis of 3-bromo-1H-pyrrolo [2, 3-b] pyridine (**6**): 1H-pyrrolo[2,3-*b*]pyridine **(1)** was dissolved in dimethylformamide (DMF) and added *N*-bromosuccinamide in DMF solution was added dropwise at ambient temperature. The reaction mixture was stirred overnight at RT. Once the reaction is complete as indicated by TLC, water was added to reaction mixture and 3-bromo-1H-pyrrolo[2,3-b]pyridine (**6**) was collected by filtration.

4.2.4. Synthesis of 3-(4-substituted-1H-1,2,3-triazol-1-yl)-1H-pyrrolo[2,3-b]pyridine (**7a-k**): 3-bromo-1*H*-pyrrolo[2,3-*b*]pyridine (**6)** (0.5 mmol, 1 equiv) was mixed with variety of alkynes (0.55mmol, 1.1equiv) 9:1 DMSO/H_2O in a 20 mL scintillation vial. To this mixture, were added L-proline (0.1 mmol, 0.2 equiv), Na_2CO_3 (0.1 mmol, 0.2 equiv), NaN_3 (0.6 mmol, 1.2 equiv), sodium ascorbate (0.05 mmol, 0.1 equiv) and $CuSO_4.5H_2O$ (0.025 mmol, 0.05 equiv). The mixture was stirred overnight at 60°C. Upon completion of the reaction (monitoredby TLC), the crude mixture was poured into water and extracted with ethyl acetate. Combined organic layers were and dried over anhydrous sodium sulphate to get the crude product. Compound was further purified by column chromatography with pet ether and ethyl acetate (15%).

4.2.4.1. 3-(4-phenyl-1H-1,2,3-triazol-1-yl)-1H-pyrrolo[2,3-b]pyridine (**7a**). White solid; yield 85%, 0.33g, m.p. 161-163° C; IR (KBr, cm^{-1}) 3310, 3025, 1655. ^{1}H NMR (400 MHz, DMSO) δ 12.89 (s, 1H), 8.71 (s, 1H), 8.27 (dd, *J* = 4.6, 1.2 Hz, 1H). 8.01 (dd, *J* = 7.9, 1.5 Hz, 2H). 7.55 (t, *J* = 7.2 Hz, 2H). 7.45 (d, *J* = 7.2 Hz, 2H). 7.15 (dd, *J* = 7.9, 4.7 Hz, 1H). 6.82 (s, 1H). ^{13}C NMR (101 MHz, $CDCl_3$) δ 148.32, 145.92, 142.86, 132.04, 131.66, 129.38, 128.69, 127.91, 126.64, 125.01, 121.21, 116.82, 101.45. ESI-MS (m/z): calcd. for $C_{15}H_{11}N_5$261.1, found 262.17 $[M + H]^+$.

4.2.4.2. 3-(4-p-tolyl-1H-1,2,3-triazol-1-yl)-1H-pyrrolo[2,3-b]pyridine (**7b**). Pale yellow solid; yield 84%, 0.35g, m.p. 117-119° C; IR (KBr, cm^{-1}) 3322, 3032, 1663. ^{1}H NMR (400 MHz, DMSO) δ 12.10 (s, 1H), 8.30 (dd, *J* = 4.6, 1.2 Hz, 1H). 8.21 (s, 1H), 7.84 (dd, *J* = 7.9, 1.5 Hz, 1H). 7.75 (d, *J* = 7.2 Hz, 2H). 7.72 (d, *J* = 7.2 Hz, 1H). 7.25 (d, *J* = 4.3 Hz, 2H). 7.17 (dd, *J* = 7.9, 4.7 Hz, 1H). 2.32 (s, 3H). ^{13}C NMR (101 MHz, $CDCl_3$) δ 147.62, 144.33, 142.86, 129.92, 128.48, 127.42, 126.89, 126.50, 126.04, 119.15, 116.82, 100.22, 87.99, 21.30. ESI-MS (m/z): calcd. for $C_{16}H_{13}N_5$275.12, found 276.19 $[M + H]^+$.

4.2.4.3. 3-(4-(4-tert-butylphenyl)-1H-1,2,3-triazol-1-yl)-1H-pyrrolo[2,3-b]pyridine (**7c**). Pale yellow solid; yield 83%, 0.40g, m.p. 121-123° C; IR (KBr, cm^{-1}) 3328, 3028, 1665. ^{1}H NMR (400 MHz, DMSO) δ 12.07 (s, 1H), 8.30 (dd, *J* = 4.6, 1.2 Hz, 1H), 8.19 (s, 1H), 7.85 (dd, *J* = 7.9, 1.5 Hz, 1H), 7.77 (d, *J* = 7.2 Hz, 2H), 7.71 (d, *J* = 7.2 Hz, 1H), 7.46 (d, *J* = 4.3 Hz, 2H), 7.18 (dd, *J* = 7.9, 4.7 Hz, 1H), 1.30 (s, 9H). ^{13}C NMR (101 MHz, DMSO) δ 149.26, 147.63, 144.23, 131.14, 131.01, 128.51, 126.89, 126.36, 126.04, 125.86, 119.16, 116.82, 100.15, 34.82, 31.50. ESI-MS (m/z): calcd. for $C_{19}H_{19}N_5$ 317.16, found 317.24 $[M + H]^+$.

4.2.4.4. 3-(4-butyl-1H-1,2,3-triazol-1-yl)-1H-pyrrolo[2,3-b]pyridine (**7d**). Brown solid; yield 79%, 0.29g, m.p. 156-157° C; IR (KBr, cm^{-1}) 3325, 3056, 1667, 1472. ^{1}H NMR (400 MHz, DMSO) δ 12.09 (s, 1H), 8.30 (dd, *J* = 4.6, 1.2 Hz, 1H), 7.84 (dd, *J* = 7.9, 1.5 Hz, 1H), 7.76 (s, 1H), 7.19 (dd, *J* = 7.9, 4.7 Hz, 1H), 7.08 (dd, *J* = 7.9, 4.7 Hz, 1H), 2.01 (t, *J* = 6.8 Hz, 3H), 1.55-1.45 (m, 6H). ^{13}C NMR (100.61 MHz, $CDCl_3$) δ 148.76, 147.36, 144.72, 142.74, 128.60, 126.89, 119.14, 116.87, 101.22, 10.25, 9.29, 8.86, 8.12. ESI-MS (m/z): calcd. for $C_{13}H_{15}N_5$241.13, found 242.21 $[M + H]^+$.

4.2.4.5. 3-(4-cyclopropyl-1H-1,2,3-triazol-1-yl)-1H-pyrrolo[2,3-b]pyridine (**7e**). Pale yellow solid; yield 69%, 0.23g, m.p. 148-149° C; IR (KBr, cm^{-1}) 3342, 3024, 1651, 1425. ^{1}H NMR (400 MHz, DMSO) δ 12.11 (s, 1H), 8.31 (dd, *J* = 4.6, 1.2 Hz, 1H). 7.85 (dd, *J* = 7.9, 1.5 Hz, 1H), 7.74 (s, 1H), 7.18 (dd, *J* = 7.9, 4.7 Hz, 1H), 7.06 (dd, *J* = 7.9, 4.7 Hz, 1H), 2.00 (tt, *J* = 7.2 Hz, *J* = 6.9 Hz, 1H), 0.92 (t, *J* = 7.2 Hz, 2H), 0.72 (t, *J* = 6.8 Hz, 2H). ^{13}C NMR (100.61

MHz, $CDCl_3$) δ 148.72, 147.62, 144.32, 142.74, 128.60, 126.89, 126.04, 119.16, 116.81, 100.26, 8.90, 8.37. ESI-MS (m/z): calcd. for $C_{12}H_{11}N_5$ 225.1, found 226.19 $[M + H]^+$.

4.2.4.6. 2-(1-(1H-pyrrolo[2,3-b]pyridin-3-yl)-1H-1,2,3-triazol-4-yl)propan-2-ol (**7f**). Pale yellow solid; yield 87%, 0.32g, m.p. 149-151° C; IR (KBr, cm^{-1}) 3420, 3336, 3054, 1676, 1450. ^1H NMR (400 MHz, DMSO) δ 12.08 (s, 1H), 8.30 (dd, *J* = 4.6, 1.2 Hz, 1H). 7.93 (dd, *J* = 7.9, 4.7 Hz, 1H), 7.83 (dd, *J* = 7.9, 4.7 Hz, 1H), 7.72 (s, 1H), 7.06 (dd, *J* = 7.9, 4.7 Hz, 1H), 6.44 (s, 1H), 1.35 (s, 6H). ^{13}C NMR (101 MHz, DMSO) δ 148.86, 147.62, 144.33, 128.48, 126.89, 126.04, 119.15, 116.82, 100.22, 87.59. 32.04. ESI-MS (m/z): calcd. for $C_{12}H_{13}N_5O$ 243.11, found 244.21 $[M + H]^+$.

4.2.4.7. 3-(1-(1H-pyrrolo[2,3-b]pyridin-3-yl)-1H-1,2,3-triazol-4-yl)propan-1-ol (**7g**). White solid; yield 73%, 0.27g, m.p. 150-152° C; IR (KBr, cm^{-1}) 3425, 3327, 3055, 1675, 1446. ^1H NMR (400 MHz, DMSO) δ 12.10 (s, 1H), 8.31 (dd, *J* = 4.6, 1.2 Hz, 1H), 7.86 (dd, *J* = 7.9, 1.5 Hz, 1H), 7.78 (s, 1H), 7.18 (dd, *J* = 7.9, 4.7 Hz, 1H), 7.09 (dd, *J* = 7.9, 4.7 Hz, 1H), 4.01 (s, 1H), 1.61-1.48 (m, 6H). ^{13}C NMR (100.61 MHz, $CDCl_3$) δ 148.32, 147.12, 144.62, 142.74, 128.65, 126.82, 119.12, 116.87, 101.22, 11.02, 10.24, 9.31. ESI-MS (m/z): calcd. for $C_{12}H_{13}N_5O$ 243.11, found 244.18 $[M + H]^+$.

4.2.4.8. Ethyl1-(1H-pyrrolo[2,3-b]pyridin-3-yl)-1H-1,2,3-triazole-4-carboxylate (**7h**). Pale yellow solid; yield 78%, 0.30g, m.p. 165-167° C; IR (KBr, cm^{-1}) 3317, 3062, 1672, 1424. ^1H NMR (400 MHz, DMSO) δ 12.08 (s, 1H), 8.30 (dd, *J* = 4.6, 1.2 Hz, 1H), 7.84 (dd, *J* = 7.9, 1.5 Hz, 1H), 7.79 (s, 1H), 7.17 (dd, *J* = 7.9, 4.7 Hz, 1H), 7.06 (dd, *J* = 7.9, 4.7 Hz, 1H), 3.78 (q,*J* = 6.4 Hz, 2H), 2.41(t, *J* = 6.2 Hz 3H). ^{13}C NMR (100.61 MHz, $CDCl_3$) δ 152.21, 148.31, 147.32, 144.48, 142.52, 128.61, 126.82, 119.13, 116.82, 101.81, 62.32, 15.32. ESI-MS (m/z): calcd. for $C_{12}H_{11}N_5O_2$ 257.09, found 258.17 $[M + H]^+$.

4.2.4.9. (1-(1H-pyrrolo[2,3-b]pyridin-3-yl)-1H-1,2,3-triazol-4-yl)methanol (**7i**). White solid; yield 83%, 0.27g, m.p. 120-121° C; IR (KBr, cm^{-1}) 3435, 3325, 3020, 1670. ^1H NMR (400 MHz, DMSO) δ 12.11 (s, 1H), 8.28 (dd, *J* = 4.6, 1.2 Hz, 1H), 7.84 (dd, *J* = 7.9, 1.5 Hz, 1H), 7.77 (s, 1H), 7.19 (dd, *J* = 7.9, 4.7 Hz, 1H), 7.08 (dd, *J* = 7.9, 4.7 Hz, 1H), 4.12 (s, 1H), 3.12 (s, 2H).

^{13}C NMR (100.61 MHz, $CDCl_3$) δ 148.32, 147.12, 144.62, 142.74, 128.65, 126.82, 119.12, 116.87, 101.22, 56.43. ESI-MS (m/z): calcd. for $C_{10}H_9N_5O$ 215.08, found 216.17 $[M + H]^+$.

4.2.4.10. 3-(4-(4-fluorophenyl)-1H-1,2,3-triazol-1-yl)-1H-pyrrolo[2,3-b]pyridine (**7j**). Brownsolid; yield 69%, 0.29g, m.p. 127-128° C; IR (KBr, cm^{-1}) 3342, 3050, 1671, 1260. ^{1}H NMR (400 MHz, DMSO) δ 12.10 (s, 1H), 8.31 (dd, *J* = 4.6, 1.2 Hz, 1H). 8.20 (s, 1H), 7.86 (dd, *J* = 7.9, 1.5 Hz, 1H). 7.73 (d, *J* = 7.2 Hz, 2H). 7.71 (d, *J* = 7.2 Hz, 1H). 7.23 (d, *J* = 4.3 Hz, 2H). 7.12 (dd, *J* = 7.9, 4.7 Hz, 1H). ^{13}C NMR (101 MHz, $CDCl_3$) δ 148.52, 144.32, 142.84, 129.97, 128.28, 127.12, 126.89, 126.50, 126.16, 119.15, 116.86, 101.22, 100.16. ESI-MS (m/z): calcd. for $C_{15}H_{10}FN_5$ 279.09, found 280.15 $[M + H]^+$.

4.2.4.11. 3-(4-(4-methoxyphenyl)-1H-1,2,3-triazol-1-yl)-1H-pyrrolo[2,3-b]pyridine (**7k**). Pale yellow solid; yield 76%, 0.33g, m.p. 165-166° C; IR (KBr, cm^{-1}) 3325, 3050, 1670, 1175. ^{1}H NMR (400 MHz, DMSO) δ 12.08 (s, 1H), 8.29 (dd, *J* = 4.6, 1.2 Hz, 1H), 8.20 (s, 1H), 7.81 (dd, *J* = 7.9, 1.5 Hz, 1H), 7.79 (d, *J* = 7.2 Hz, 2H), 7.71 (d, *J* = 7.2 Hz, 1H), 7.22 (d, *J* = 4.3 Hz, 2H), 7.18 (dd, *J* = 7.9, 4.7 Hz, 1H), 3.82 (s, 3H). ^{13}C NMR (101 MHz, $CDCl_3$) δ 147.59, 144.31, 142.82, 129.54, 128.67, 127.40, 126.83, 126.71, 126.04, 119.15, 116.81, 101.21, 100.43, 56.38. ESI-MS (m/z): calcd. for $C_{16}H_{13}N_5O$ 291.11, found 292.18 $[M + H]^+$.

4.3. *Biology*

The cell lines, A549-lung (doubling time: 22 h), HeLa-cervix (doubling time: 19 h) and MDA MB 231-breast cancer (doubling time: 27 h) which were used in this study were procured from American Type Culture Collection (ATCC), United States. In addition, WPMY-1 was employed as a normal prostatic myofibroblast cell line. The synthesized test compounds were evaluated for their *in vitro* antiproliferative activity in these three different human cancer cell lines. A protocol of 48 h continuous drug exposure was used, and a SRB cell proliferation assay was used to estimate cell viability or growth. All the cell lines were grown in Dulbecco's modified Eagle's medium (containing 10% FBS in a humidified atmosphere of 5% CO_2 at 37 °C). Cells were trypsinized when sub-confluent from T25 flasks/60 mm dishes and seeded in 96-well plates in 100 μL aliquots at plating densities depending on the doubling time of individual cell lines. The microtiter plates were incubated at 37 °C, 5% CO_2, 95% air, and 100% relative

humidity for 24 h prior to addition of experimental drugs and were incubated for 48 h with different doses (0.01, 0.1, 1, 10 and 100µM) of prepared derivatives**.** After 48 h incubation at 37 °C, cell monolayers were fixed by the addition of 10% (wt/vol) cold trichloroacetic acid and incubated at 4 °C for 1 h and were then stained with 0.057% SRB dissolved in 1% acetic acid for 30 min at room temperature. Unbound SRB was washed with 1% acetic acid. The protein – bound dye was dissolved in 10 mM Tris base solution for OD was measured at 510 nm using a microplate reader (Enspire, Perkin Elmer, USA). Using the seven absorbance measurements [time zero, (Tz), control growth, (C), and test growth in the presence of drug at the five concentration levels (Ti)], the percentage growth was calculated at each of the drug concentrations levels. Percentage growth inhibition was calculated as:

[(Ti-Tz)/(C-Tz)] x 100 for concentrations for which Ti>/=Tz

[(Ti-Tz)/Tz] x 100 for concentrations for which Ti<Tz.

The dose response parameter, GI_{50} was calculated for each experimental agent. Growth inhibition of 50 % (GI_{50}) was calculated from [(Ti-Tz)/(C-Tz)] x 100 = 50, which is the drug concentration resulting in a 50% reduction in the net protein increase (as measured by SRB staining) in control cells during the drug incubation. Values were calculated for this parameter if the level of activity is reached; however, if the effect is not reached or is exceeded, the value for that parameter was expressed as greater or less than the maximum or minimum concentration tested.

4.4. *Western blot*

Hela cells were seeded in 6-well plates at 0.2 million cells per well in complete growth medium. Following treatment of cells with **5d** and cirtzonib for duration of 24 h, cells were washed with PBS and subsequently whole cell lystes were prepared in Laemmli's sample buffer. Samples were immediately heated to 95 °C for 3 min. Equal volumes of samples were run on an SDS-10% polyacrylamide gel and were transferred to a nitrocellulose membrane employing semidry transfer at 50 mA for 1 h. Blots were probed with mouse anti-human p53 and α-tubulin, diluted to 1 : 5000 ml (Sigma) and stained with the rabbit anti-mouse secondary antibody coupled with horseradish peroxidase diluted to 1 : 5000 ml (Sigma). Bands were visualized using an enhanced chemiluminescence protocol (Pierce) and radiographic film (Kodak).

Acknowledgments

We acknowledge the financial support from Department of Biotechnology (DBT) (BT/PR4801/MED/29/370/2012), Government of India, New Delhi. N.S. thanks UGC, New Delhi for the award of senior research fellowship.

References:

[1]. M. Alvarez, D.E. Fernandez, J.A. Joule, Synthesis of 3-aryl- and 3-heteroaryl-7-azaindoles Synthesis, Synthesis-S. 4 (1999) 615-620.

[2]. L.D. Arnold, X. Chen, H. Dong, A. Garton, M.J. Mulvihill, C.P.S. Smith, G.H. Thomas, T.M. Krulle, J. Wang, US Patent 20070208053 (2007).

[3]. P.J. Cox, T.N. Majid, S. Amendola, S.D. Deprets, C. Edlin, J.Y.Q. Lai, A.D. Morley, USPatent 20040198737 (2004).

[4]. H.J. Dyke, S. Price, K. Williams, US Patent 20100216768 (2010).

[5]. G.N. Anilkumar, S.B. Rosenblum, S. Venkatraman, F.G. Njoroge, J.A. Kozlowski, US Patent 20100239527 (2010).

[6]. M.P. Clark, M.W. Ledeboer, I. Davies, R.A. Byrn, S.M. Jones, E. Perola, A. Tsai, M. Jacobs, K.N. Addae, U.K. Bandarage, M.J. Boyd, R.S. Bethiel, J.J. Court, H. Deng, J.P. Duffy, W.A. Dorsch, L.J. Farmer, H. Gao, W. Gu, K. Jackson, D.H. Jacobs, J.M. Kennedy, B. Ledford, J. Liang, F. Maltais, M. Murcko, T. Wang, M.W. Wannamaker, H.B. Bennett, J.R. Leeman, C. McNeil, W.P. Taylor, C. Memmott, M. Jiang, R. Rijnbrand, C. Bral, U. Germann, A. Nezami, Y. Zhang, F.G. Salituro, Y.L. Bennani, P.S. Charifson, Discovery of a Novel, First-in-Class, Orally Bioavailable Azaindole Inhibitor (VX-787) of Influenza PB2, J. Med. Chem. 57 (2014) 6668−6678.

[7]. V.S. Goodfellow, C.J. Loweth, S.B. Ravula, T. Wiemann, T. Nguyen, Y. Xu, D.E. Todd, D. Sheppard, S. Pollack, O. Polesskaya, D.F. Marker, S. Dewhurst, H.A. Gelbard. Discovery, Synthesis, and Characterization of an Orally Bioavailable, Brain Penetrant Inhibitor of Mixed Lineage Kinase 3, J. Med. Chem. 56 (2013) 8032–8048.

[8]. S. Lee, H. Lee, J. Kim, S. Lee, S.J. Kim, B.S. Choi, S.S. Hong, S. Hong. Development and Biological Evaluation of Potent and Selective C‑KITD816V Inhibitors, J. Med. Chem. 57 (2014) 6428−6443.

[9]. A.W. Hung, H.L. Silvestre, S. Wen, A. Ciulli, T.L. Blundell, C. Abell, Application of fragment growing and fragment linking to the discovery of inhibitors of *Mycobacterium tuberculosis* pantothenate synthetase, Angew. Chem. Int. Ed. 48 (2009) 8452-8456.

[10]. S. Hong, S. Lee, B. Kim, H. Lee, S.S. Hong, S. Hong, Discovery of new azaindole-based PI3Ka inhibitors: Apoptotic and antiangiogenic effect on cancer cells, Bioorg. Med. Chem. Lett. 20 (2010) 7212–7215.

[11]. S. Hong, J. Kim, J.H. Seo, K.H. Jung, S.S. Hong, S. Hong, Design, Synthesis, and Evaluation of 3,5-Disubstituted 7-Azaindoles as Trk Inhibitors with Anticancer and Antiangiogenic Activities, J. Med. Chem. 55 (2012) 5337−5349.

[12]. C. Marminon, A. Pierre, B. Pfeiffer, V.P. rez, S. Leonce, P. Renard, M. Prudhommea, Syntheses and Antiproliferative Activities of Rebeccamycin Analogues Bearing Two 7-Azaindole Moieties, Bioorg. Med. Chem. 11 (2003) 679–687.

[13]. P. Starha, Z. Travnicek, A. Popa, I. Popa, T. Muchova, V. Brabec, How to modify 7-azaindole to form cytotoxic Pt(II) complexes: Highly *in vitro* anticancer effective cisplatin derivatives involving halogeno-substituted 7-azaindole, J. Inorg. Biochem. 115 (2012) 57-63.

[14]. T. Muchova, J. Pracharova, P. Starha, R. Olivova, O. Vrana, B. Benesova, B J. Kasparkova, Z. Travnicek, V. Brabec, Insight into the toxic effects of cisdichloridoplatinum (II) complexes containing 7-azaindole halogeno derivatives in tumor cells, J. Biol. Inorg. Chem. 18 (2013) 579-589.

[15]. J. Pracharova, T. Saltarella, T.R. Muchova, S. Scintilla, V. Novohradský, O. Novakova, F.P. Intini, C. Pacifico, G. Natile, P. Ilik, V. Brabec, J. Kasparkova, Novel antitumor cisplatin and transplatin derivatives containing 1-methyl-7-azaindole: synthesis, characterization and cellular responses, J. Med. Chem. *58 (*2015) 847–859.

[16]. Y. Tong, K.D. Stewart, A.S. Florjancic, J.E. Harlan, P.J. Merta, M. Przytulinska, N. Soni, K.K. Swinger, H. Zhu, E.F. Johnson, A.R. Shoemaker, T.D. Penning, Azaindole-Based Inhibitors of Cdc7 Kinase: Impact of the Pre-DFG Residue, Val 195, ACS Med. Chem. Lett. 4 (2013) 211−215.

[17]. K. Bousset, J.F. Diffley, The Cdc7 protein kinase is required for origin firing during S phase, Genes Dev. 12 (1998) 480−490.

[18]. W. Jiang, D. McDonald, T.J. Hope, T. Hunter, Mammalian Cdc7-Dbf4 protein kinase complex is essential for initiation of DNA replication, EMBO J. 18 (1999) 5703−5713.

[19]. H. Kumagai, N. Sato, M. Yamada, D. Mahony, W. Seghezzi, E. Lees, K. Arai, H. Masai, A novel growth- and cell cycle regulated protein, ASK, activates human Cdc7-related kinase and is essential for G1/S transition in mammalian cells, Mol. Cell. Biol. 19 (1999) 5083−5095.

[20]. A. Montagnoli, R. Bosotti, F. Villa, M. Rialland, D. Brotherton, C. Mercurio, J. Berthelsen, C. Santocanale, Drf1, a novel regulatory subunit for human Cdc7 kinase, EMBO J. 2 (2002) 3171−3181.

[21]. A. Ermoli, A. Bargiotti, M.G. Brasca, A. Ciavolella, N. Colombo, G. Fachin, A. Isacchi, M. Menichincheri, A. Molinari, A. Montagnoli, A. Pillan, S. Rainoldi, F.R. Sirtori, F. Sola, S. Thieffine, M. Tibolla, B. Valsasina, D. Volpi, C. Santocanale, E. Vanotti, Cell Division Cycle 7 Kinase Inhibitors: 1H-Pyrrolo[2,3-b]pyridines, Synthesis and Structure-Activity Relationships, J. Med. Chem. 52 (2009) 4380–4390.

[22]. Y.S. Tung, M.S. Coumar, Y.S. Wu, H.Y. Shiao, J.Y. Chang, J.P. Liou, P. Shukla, C.W. Chang, C.Y. Chang, C.C. Kuo, T.K. Yeh, C.Y. Lin, J.S. Wu, S.Y. Wu, C.C. Liao, H. P. Hsieh, S.H, Strategy: Synthesis and Biological Evaluation of 5,6-Fused Bicyclic Heteroaromatics To Identify Orally Bioavailable Anticancer Agents, J. Med. Chem. 54 (2011) 3076–3080.

[23]. E. Wahlberg, T. Karlberg, E. Kouznetsova, N. Markova, A. Macchiarulo, A.G. Thorsell, E. Pol, A. Frostell, T. Ekblad, D. Oncu, B. Kull, G.M. Robertson, R. Pellicciari, H. Schuler, J. Weigelt, Family-wide chemical profiling and structural analysis of PARP and tankyrase inhibitors, Nat. Biotechnol. 30 (2012) 283-288.

[24]. M. Javle, N.J. Curtin, The role of PARP in DNA repair and its therapeutic exploitation, Br. J. Cancer 2011, 105, 1114-1122.

[25]. R. Cincinelli, L. Musso, L. Merlini, G. Giannini, L. Vesci, F.M. Milazzo, N. Carenini, P. Perego, S. Penco, R. Artali, F. Zunino, C. Pisano, S. Dallavalle, 7-Azaindole-1-carboxamides as a new class of PARP-1 inhibitors, Bioorg. Med. Chem. 22 (2014) 1089–1103.

[26]. G. Chev, C. Bories, B. Fauvel, F. Picot, A. Tible, B. D. Cazals, O. Loget, A. Yasri, De novo design, synthesis and pharmacological evaluation of new azaindole derivatives as dual inhibitors of Abl and Src kinases, Med. Chem. Commun. 3 (2012) 788-800.

[27]. C.H. Tseng, Y.L. Chen, S.H. Yang, S.I. Peng, C.M. Cheng, C.H. Han, S.R. Lin, C.C. Tzeng, Synthesis and antiproliferative evaluation of certain iminonaphtho[2,3-b]furan derivatives, Bioorg. Med. Chem. 18 (2010) 5172−5182.

[28]. T.C. Wang, I.L. Chen, P.J. Lu, C.H. Wong, C.H. Liao, K.C. Tsiao, K.M. Chang, Y.L. Chen, C.C. Tzeng, Synthesis, antiproliferative, and antiplatelet activities of oxime- and methyloximecontaining flavone and isoflavone derivatives, Bioorg. Med. Chem. 13 (2005) 6045−6053.

[29]. C.H. Tseng, Y.L. Chen, P.J. Lu, C.N. Yang, C.C. Tzeng, Synthesis and antiproliferative evaluation of certain indeno[1,2-c]quinoline derivatives, Bioorg. Med. Chem. 16 (2008) 3153−3162.

[30]. N.G. Aher, V.S. Pore, N.N. Mishra, A. Kumar, P.K. Shukla, A. Sharma, M.K. Bhat, Synthesis and antifungal activity of 1,2,3-triazole containing fluconazole analogues, Bioorg. Med. Chem. Lett. 19 (2009) 759-763.

[31]. S. Yu, N. Wang, X. Chai, B. Wang, H. Cui, Q. Zhao, Y. Zou, Q. Sun, Q. Meng, Q. Wu, Synthesis and antifungal activity of the novel triazole derivatives containing 1,2,3-triazole fragment, Arch. Pharmacal. Res. 36 (2013) 1215-1222.

[32]. J.A. Demaray, J.E. Thuener, M.N. Dawson, S.J. Sucheck, Synthesis of triazole-oxazolidinones via a one-pot reaction and evaluation of their antimicrobial activity, Bioorg. Med. Chem. Lett. 18 (2008) 4868-4871.

[33]. X.L. Wang, K. Wan, C.H. Zhou, Synthesis of novel sulfanilamide-derived 1,2,3-triazoles and their evaluation for antibacterial and antifungal activities, Eur. J. Med. Chem. 45 (2010) 4631-4639.

[34]. D.R. Buckle, D.J. Outred, C.J.M. Rockell, H. Smith, B.A. Spicer, Studies on v-triazoles. 7. Antiallergic 9-oxo-1H,9H-benzopyrano[2,3-d]-v-triazoles, J. Med. Chem. 26 (1983) 251-254.

[35]. R.D. Simone, M.G. Chini, I. Bruno, R. Riccio, D. Mueller, O. Werz, G. Bifulco, Structure-Based Discovery of Inhibitors of Microsomal Prostaglandin E_2Synthase−1, 5-

Lipoxygenase and 5-Lipoxygenase-Activating Protein: Promising Hits for the Development of New Anti-inflammatory Agents, J. Med. Chem. 54 (2011) 1565-1575.

[36]. K. Ohmoto, T. Yamamoto, T. Horiuchi, H. Imanishi, Y. Odagaki, K. Kawabata, T. Sekioka, Y. Hirota, S. Matsuoka, H. Nakai, M. Toda, J.C. Cheronis, L.W. Spruce, A. Gyorkos, M. Wieczorek, Design and synthesis of new orally active nonpeptidic inhibitors of human neutrophil elastase, J. Med. Chem. 43 (2000) 4927-4929.

[37]. H.A. Stefani, N.C.S. Silva, F. Manarin, D.S. Lüdtke, J.Z. Schpector, L.S. Madureira, E.R.T. Tiekink, Synthesis of 1,2,3-triazolylpyranosides through click chemistry reaction, Tetrahedron Lett. 53 (2012) 1742-1747.

[38]. P. Singh, R. Raj, V. Kumar, M.P. Mahajan, P.M.S. Bedi, T. Kaur, A.K. Saxena, 1,2,3-Triazole tethered β-lactam-Chalcone bifunctional hybrids: Synthesis and anticancer evaluation, Eur. J. Med. Chem. 47 (2012) 594-600.

[39]. Y.C. Duan, Y.C. Ma, E. Zhang, X.J. Shi, M.M. Wang, X.W. Ye, H.M. Liu, Design and synthesis of novel 1,2,3-triazole-dithiocarbamate hybrids as potential anticancer agents, Eur. J. Med. Chem. 62 (2013) 11-19.

[40]. Y. C. Duan, Y.C. Zheng, X.C. Li, M.M. Wang, X.W. Ye, Y.Y. Guan, G.Z. Liu, J.X. Zheng, H.M. Liu, Design, synthesis and antiproliferative activity studies of novel 1,2,3-triazole-dithiocarbamate-urea hybrids, Eur. J. Med. Chem. 64 (2013) 99-110.

[41]. N. Ahmed, N.K. Konduru, S. Ahmad, M. Owais, Design, synthesis and antiproliferative activity of functionalized flavone-triazole-tetrahydropyran conjugates against human cancer cell lines, Eur. J. Med. Chem. 82 (2014) 552-564.

[42]. L.Y. Ma, L.P. Pang, B. Wang, M. Zhang, B. Hu, D.Q. Xue, K.P. Shao, B.L. Zhang, Y. Liu, E. Zhang, H.M. Liu, Design and synthesis of novel 1,2,3-triazole-pyrimidine hybrids as potential anticancer agents, Eur. J. Med. Chem. 86 (2014) 368-380.

[43]. X. Cheng, K.H. Merz, S. Vatter, J. Christ, S. Wölfl, G. Eisenbrand 7,7[1]-Diazaindirubin—A small molecule inhibitor of casein kinase 2in vitro and in cells, Bioorg. Med. Chem. 22 (2014) 247-255.

[44]. H. Jia, G. Dai, J. Weng, Z. Zhang, Q. Wang, F. Zhou, L. Jiao, Y. Cui, Y. Ren, S. Fan, J. Zhou, W. Qing, Y. Gu, J. Wang, Y. Sai, W. Su, Discovery of (*S*)-1-(1-(Imidazo[1,2-*a*]pyridin-6-yl)ethyl)-6-(1-methyl-1*H*-pyrazol-4-yl)-1H-[1,2,3]triazolo[4,5-*b*]pyrazine (Volitinib) as a Highly Potent and Selective Mesenchymal–Epithelial Transition Factor

(c-Met) Inhibitor in Clinical Development for Treatment of Cancer, J. Med. Chem. 57 (2014) 7577-7589.

[45]. P. Talukder, S. Chen, C.T. Liu, E.A. Baldwin, S.J. Benkovic, S.M. Hecht, Tryptophan-based fluorophores for studying protein conformational changes, Bioorg. Med. Chem. 22 (2014) 5924–5934.

[46]. Z. Guidong, B.G. Virajkumar, R.S. Alex, D.P. Thomas, G. Jianchun, US Patent 2011130481 (2011).

[47]. B. Antonsson, Mitochondria and the Bcl-2 family proteins in apoptosis signaling pathways, Mol. Cell Biochem. 256-257 (2004) 141-155.

[48]. T. Taguchi, Y. Kato, Y. Baba, G. Nishimura, Y. Tanigaki, C. Horiuchi, I. Mochmatsu, M. Tsukuda, Protein levels of p21, p27, cyclin E and Bax predict sensitivity to cisplatin and paclitaxel in head and neck squamous cell carcinomas, Oncol. Rep. 11 (2004) 421-426.

[49]. P. Skehan, R. Storeng, D. Scudiero, A. Monks, J. McMahon, D. Vistica, J.T. Warren, H. Bokesch, S. Kenney, M.R. Boyd, New colorimetric cytotoxicity assay for anticancer-drug screening, J. Natl. Cancer. Inst. 82 (1990) 1107-1112.

[50]. L.V. Rubinstein, R.H. Shoemaker, K.D. Paull, R.M. Simon, S. Tosini, P. Skehan, D.A. Scudiero, A. Monks, M.R. Boyd, Comparison of in vitro anticancer-drug screening data generated with a tetrazolium assay versus a protein assay against a diverse panel of human tumor cell lines, J. Natl. Cancer Inst. 82 (1990) 1113-1118.

[51]. R. Fukuda, S. Takenaka, M. Takagi, Metal ion assisted DNA-intercalation of crown ether-linked acridine derivatives, J. Chem. Soc. Chem. Commun. 1 (1990) 1028– 1030.

[52]. J. Kapuscinski, Z. Darzynkiewicz, Interactions of antitumor agents ametantrone, and mitoxantrone (novatrone) with double-stranded DNA, Biochem. Pharmacol. 34 (1985) 4203–4213.

[53]. X.J. Dang, M.Y. Nie, J. Tong, H.L. Li, Inclusion of the parent molecules of some drugs with β-cyclodextrin studied by electrochemical and spectrometric methods, J. Electroanal. Chem. 448 (1998) 61–67.

[54]. N. Li, Y. Ma, C. Yang, L. Guo, X.R. Yang, Interaction of anticancer drug mitoxantrone with DNA analyzed by electrochemical and spectroscopic methods, Biophys. Chem. 116 (2005) 199–205.

[55]. N. Chitrapriya, T. Sathiya Kamatchi, M. Zeller, H. Lee, K. Natarajan. Synthesis, spectroscopic, crystal structure and DNA binding of Ru(II) complexes with 2-hydroxy-benzoic acid [1-(4-hydroxy-6-methyl-2-oxo-2H-pyran-3-yl)-ethylidene]-hydrazide, Spectro. Acta. Part. A, Mol. Biomol. Spect. 81 (2011) 128–134.

[56]. J. R. Lakowicz, G. Webber, Quenching of fluorescence by oxygen. A probe for structural fluctuations in macromolecules, Biochemistry. 12 (1973) 4161-4170.

[57]. J.F. Lutz, Z. Zarafshani, Efficient construction of therapeutics, bioconjugates, biomaterials and bioactive surfaces using azide-alkyne "click" chemistry, Adv. Drug Delivery Rev. 60 (2008) 958-970.

[58]. M.D. Best, Click chemistry and bioorthogonal reactions: unprecedented selectivity in the labeling of biological molecules. Biochemistry. 48 (2009) 6571-6584.

Figure 1: Oxime containing anticancer compounds [27-29].

Figure 2: Examples of some 1,2,3-triazole based anticancer agents [39,41,42].

Figure 3: Amino acid interaction pattern of **7f, 7g, 7i** and **crizotinib.**

Figure 4: The Absorption spectra of Compound **5d**-CtDNA system: nm, [Compound] = 0.015× 10^{-5} M. Arrow shows the absorption intensity changes upon increasing CtDNA concentration.

Figure 5: Plot of [DNA]/(εa − εf) *vs* [DNA] for the titration of DNA with compound **5d** and solid line is linear fitting of the data.

Figure 6: The Fluoroscence spectra of DNA-EB system: ex =500nm, em = 520-720 nm, [Compound]= 0-1.64 × 10^{-5} M. CtDNA (------line). Arrow shows the emission intensity changes upon increasing compound (**5d**) concentration.

Figure 7: Stern-Volmer plot of the fluorescence titration data of the compound (**5d**). (Plots of I_0/I versus [Compound **5d**]).

Figure 8: Immunoblot for p53 in **5d** treated cells: HeLa cells were treated with compound **5d** at a concentrations of 5 and 10 mM for 24 h. Later, whole cell lysates were prepared and protein levels of p53 were determined with suitable antibody. Tubulin was used as a loading control. DMSO was used as a vehicle control.

Scheme 1: Reagents and conditions: (a) HMTA, CH_3COOH:H_2O, (b) Propargyl bromide, K_2CO_3, DMF, RT (c) Hydroxylamine hydrochloride, Ethanol (d) various aromatic azides, $CuSO_4.5H_2O$, Sodium ascorbate, *t*-BuOH:H_2O (1:1), 2h.

Scheme 2: Reagents and conditions: (a) *N*-Bromosuccinamide, DMF, RT (b) Various alkynes, sodium azide, L-proline, Na_2CO_3, $CuSO_4.5H_2O$, Sodium Ascorbate, DMSO:H_20 (9:1).

Table 1: Antiproliferative activity ($^aGI_{50}$μM) and docking scores of compounds (**5a-u** and **7a-k)**.

Table 1: Antiproliferative activity ([a]GI_{50} μM) and docking scores of compounds (**5a-u and 7a-k)**

S.No	Entry	R	[b]A549	[c]HeLa	[d]MDA-MB-231	[e]WPMY	Docking Score
1	5a	4-CH_3CH_2-	3.94±0.32	1.84±0.02	0.46±0.02	9.27±0.8	-5.161
2	5b	3-CF_3,4-Br	0.33±0.01	1.35±0.13	1.3±0.09	5.8±0.3	-4.412
3	5c	4-Br	0.7±0.01	0.93±0.02	**0.25±0.03**	4.5±0.8	-5.216
4	5d	4-CF_3	**0.12±0.01**	0.79±0.05	0.63±0.02	5.2±0.9	-5.522
5	5e	4-Cl	1.12±0.08	0.9±0.01	**0.13±0.01**	4.9±0.2	-5.104
6	5f	4-F	0.3±0.02	0.86±0.02	1.22±0.07	5.0±0.1	------
7	5g	4-OCH_3	1.82±0.07	0.81±0.01	1.51±0.05	6.2±0.1	-6.37
8	5h	4-NO_2	**0.24±0.01**	0.92±0.01	2.5±0.12	4.1±0.4	-5.207
9	5i	4-I	0.63±0.02	1.19±0.09	1.6±0.02	5.1±0.2	-5.628
10	5j	2-F	1.2±0.09	1.18±0.11	1.2±0.08	6.8±0.7	-5.072
11	5k	2-Cl	**0.16±0.04**	0.68±0.02	6.3±0.23	9.8±0.4	-5.618
12	5l	2-Br	2.69±0.07	0.39±0.05	3.0±0.01	10.3±0.2	-6.332
13	5m	2-I	1.17±0.08	0.76±0.02	**0.13±0.01**	4.7±0.6	-5.145
14	5n	3-OCH_3	0.78±0.04	0.79±0.03	**0.23±0.02**	4.0±0.2	-4.833
15	5o	2-NO_2	0.95±0.02	1.14±0.03	0.41±0.01	4.8±0.9	-5.399
16	5p	3-Cl,4-F	0.83±0.03	0.95±0.02	2.7±0.06	5.7±0.8	-5.378
17	5q	3,4-di-Cl	1.17±0.06	1.05±0.09	**0.25±0.02**	4.5±0.5	-5.043
18	5r	3,4-di-F	0.95±0.02	1.39±0.1	9.3±0.9	14.7±0.7	-5.471
19	5s	3,4-di-OCH_3	0.91±0.01	1.91±0.07	**0.14±0.02**	5.7±0.3	-4.728
20	5t	3,4-di-CH_3	0.92±0.01	0.97±0.04	6.98±0.56	13.4±0.9	-5.476
21	5u	3,4-methylene dioxy	0.98±0.03	1.0±0.03	1.57±0.08	4.7±0.2	-5.5
22	7a	C_6H_5-	0.98±0.02	0.92±0.01	9.84±0.59	15.8±0.9	-7.429
23	7b	4-$CH_3C_6H_4$-	0.33±0.01	0.89±0.03	6.22±0.17	13.3±0.7	-7.414
24	7c	4-$C(CH_3)_3$-C_6H_4-	0.4±0.01	1.03±0.02	0.48±0.02	3.9±0.4	-7.185

25	7d	$CH_3(CH_2)_3$-	0.83±0.02	1.86±0.09	15.3±1.8	25.9±0.7	-7.971
26	7e	Cyclopropyl	0.61±0.01	1.32±0.08	4.0±0.3	9.1±0.6	-7.367
27	7f	$OH(CH_3)_2C$-	0.82±0.01	0.9±0.01	8.4±0.53	17.3±0.1	**-8.381**
28	7g	$OH(CH_2)_2CH_2$-	0.81±0.009	0.95±0.02	0.69±0.04	4.4±0.5	**-8.18**
29	7h	CH_3CH_2OCO-	1.3±0.16	0.88±0.05	2.59±0.25	7.7±0.5	-7.906
30	7i	OH-CH_2-	1.73±0.07	0.93±0.02	4.69±0.5	9.8±0.8	**-8.663**
31	7j	4-F-C_6H_4-	**0.18±0.02**	0.7±0.02	**0.25±0.02**	6.2±0.2	-7.47
32	7k	4-OCH_3-C_6H_4-	**0.17±0.01**	0.83±0.03	0.45±0.01	8.8±0.2	-7.267
	Crizotinib						-8.123
	Doxorubicin		<0.01	0.09±0.001	<0.01	<0.01	
	Paclitaxel		<0.01	0.023±0.002	<0.01	<0.01	

[a]50% of growth inhibition, [b]Lung cancer cell line, [c]Cervical cancer cell line, [d]Breast cancer cell line, [e]Normal prostate cell line

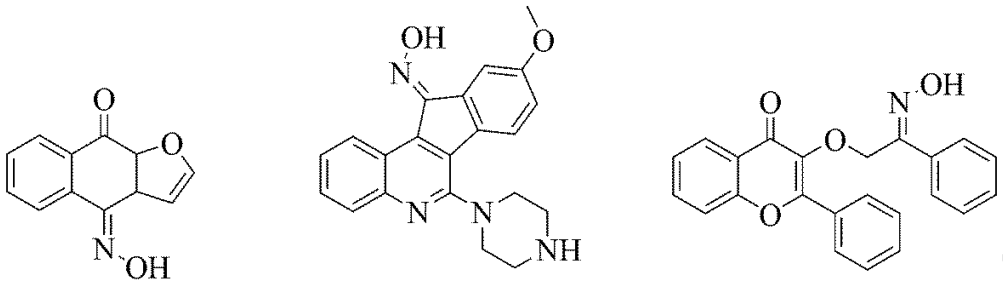

$GI_{50} = 0.82 \pm 0.02\ \mu M$ $GI_{50} = 1.74 \pm 0.47\ \mu M$ $GI_{50} = 1.8 \pm 0.20\ \mu M$

Figure 1: Oxime containing anticancer compounds [27-29].

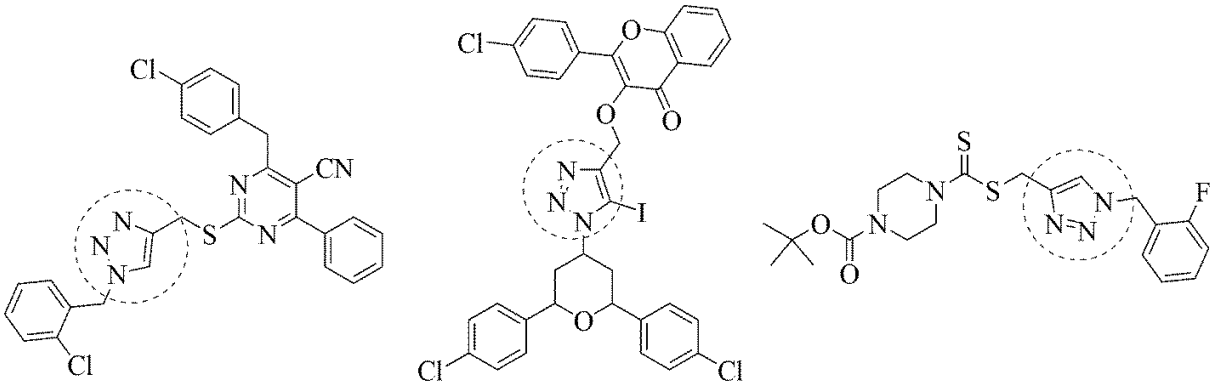

Figure 2: Examples of some 1,2,3-triazole based anticancer agents [39,41,42].

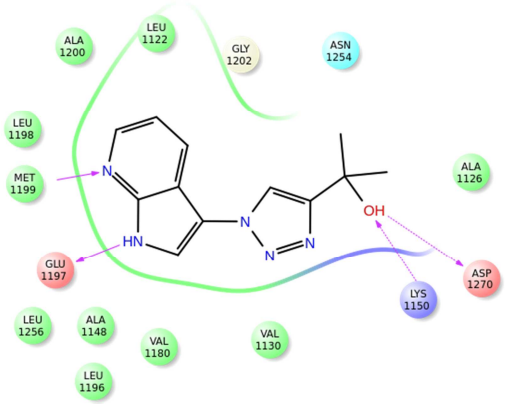

7f

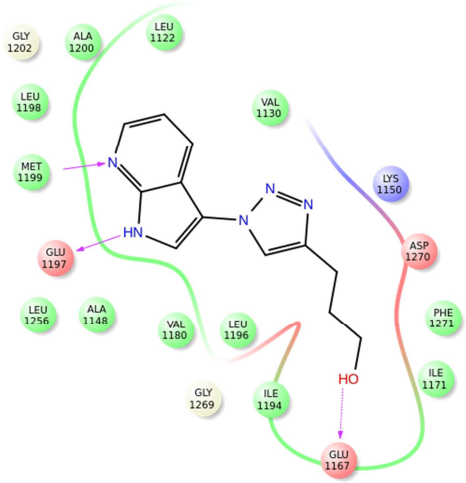

7g

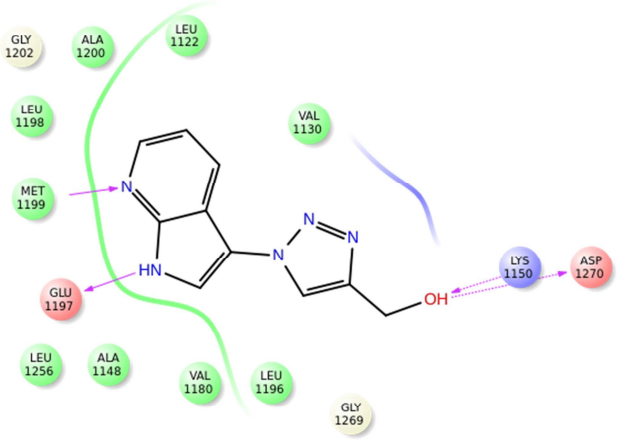

7i

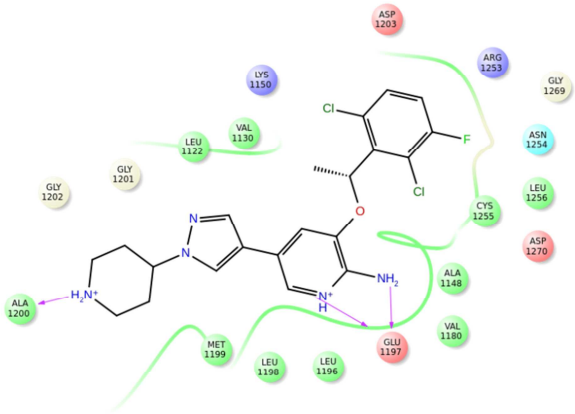

Crizotinib

Figure 3: Amino acid interaction pattern of **7f, 7g, 7i** and **crizotinib.**

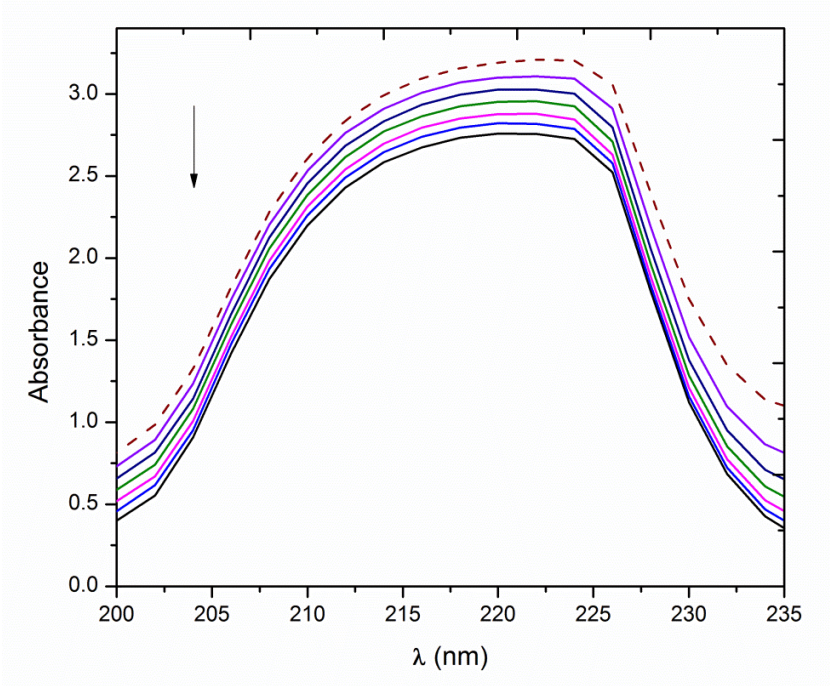

Figure 4: The Absorption spectra of Compound **5d**-CtDNA system: nm, [Compound] = 0.015× 10^{-5} M. Arrow shows the absorption intensity changes upon increasing CtDNA concentration.

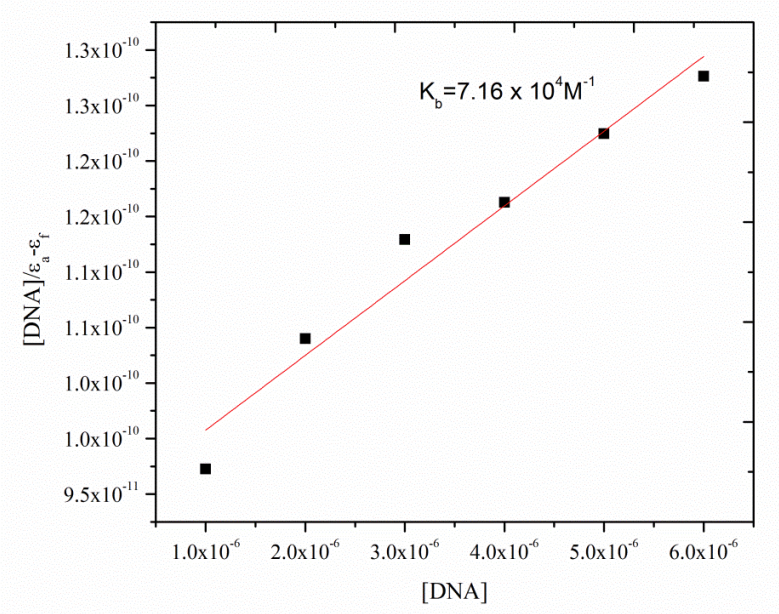

Figure 5: Plot of [DNA]/(εa − εf) *vs* [DNA] for the titration of DNA with compound **5d** and solid line is linear fitting of the data

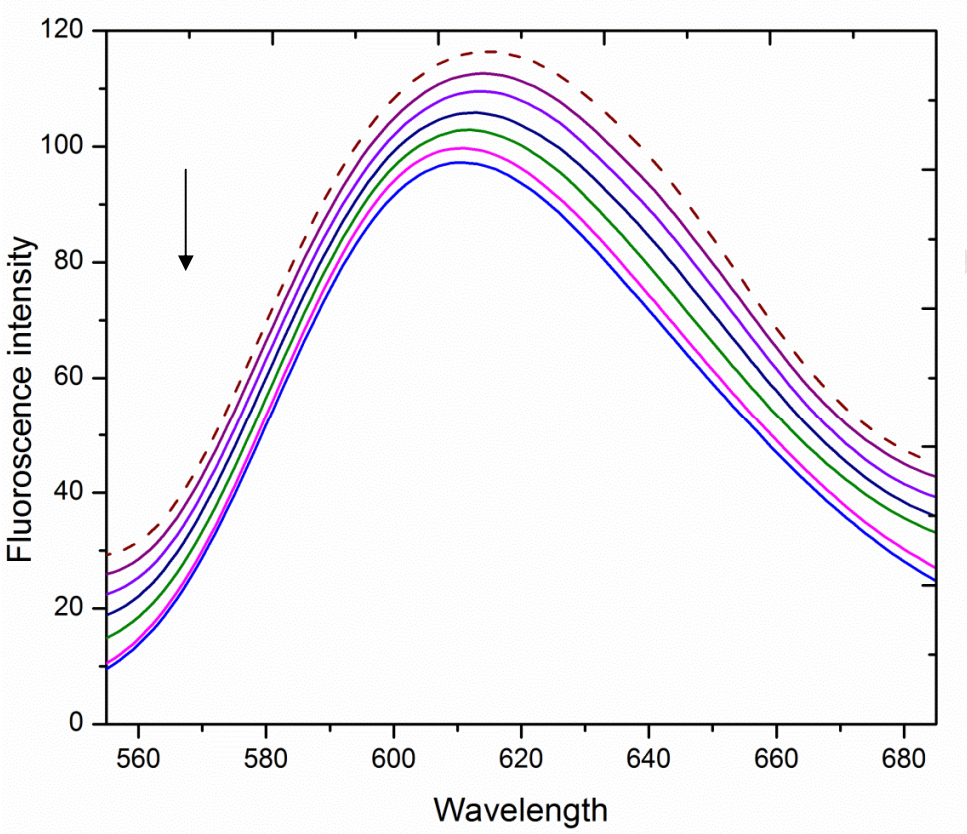

Figure 6: The Fluoroscence spectra of DNA-EB system: ex =500nm, em = 520-720 nm, [Compound] = 0-1.64 × 10^{-5} M. CtDNA (------line). Arrow shows the emission intensity changes upon increasing compound (**5d**) concentration.

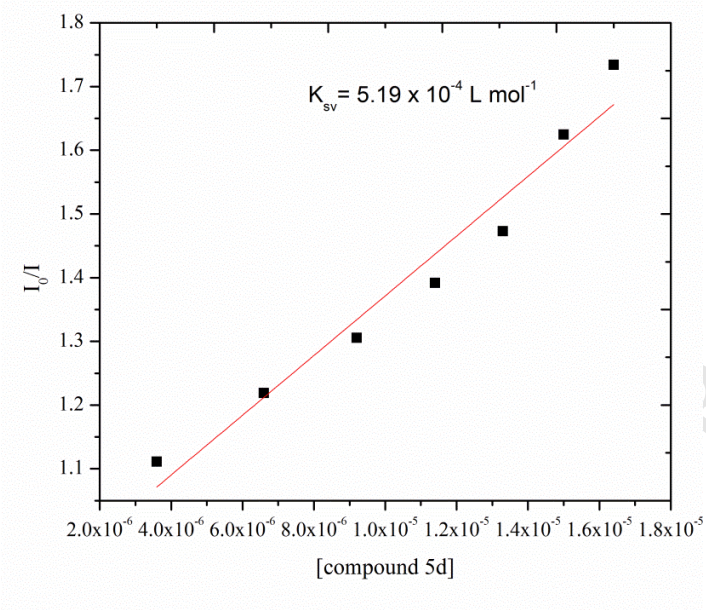

Figure 7: Stern-Volmer plot of the fluorescence titration data of the compound (**5d**). (Plots of I_0/I versus [Compound **5d**]).

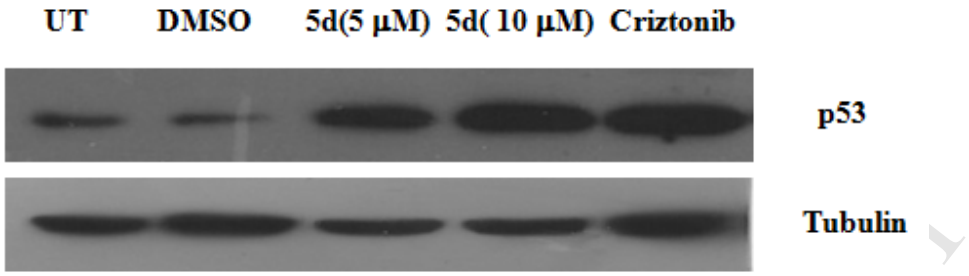

Figure 8: Immunoblot for p53 in 5d treated cells: HeLa cells were treated with compound **5d** at a concentrations of 5 and 10 µM for 24 h. Later, whole cell lysates were prepared and protein levels of p53 were determined with suitable antibody. Tubulin was used as loading control. DMSO was used as vehicle control.

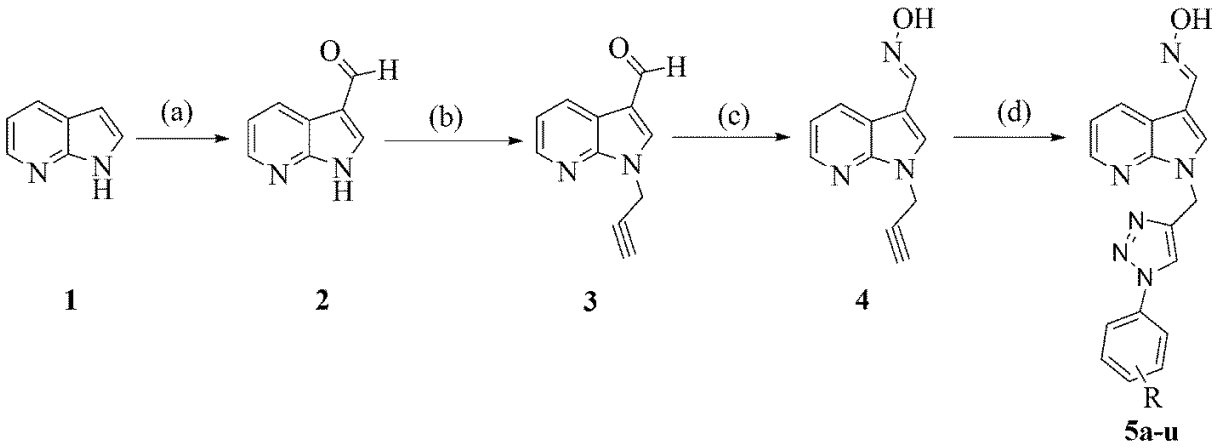

Scheme 1: Reagents and conditions: (a) HMTA, $CH_3COOH:H_2O$, (b) Propargyl bromide, K_2CO_3, DMF, RT (c) Hydroxylamine hydrochloride, Ethanol (d) various aromatic azides, $CuSO_4.5H_2O$, Sodium ascorbate, *t*-$BuOH:H_2O$ (1:1), 2h.

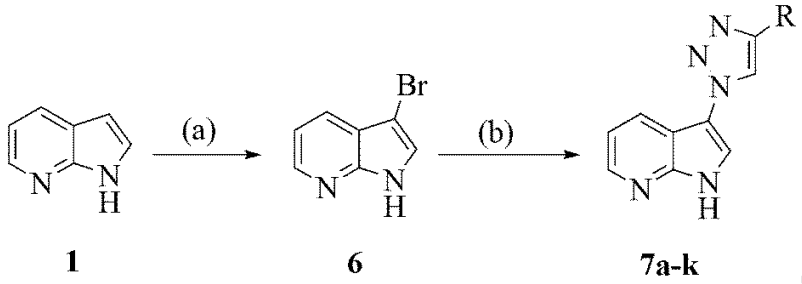

Scheme 2: Reagents and conditions: (a) N-Bromosuccinamide, DMF, RT (b) Various alkynes, sodium azide, L-proline, Na_2CO_3, $CuSO_4.5H_2O$, Sodium Ascorbate, DMSO: H_2O (9:1).

- New 7-azaindole analogues were synthesized and evaluated for anticancer activity.
- Cytotoxic evaluation carried against A549, HeLa and MDA MB-231 cancer cell lines.
- **5c**, **5d**, **5e**, **5h**, **5k**, **5m**, **5n**, **5q**, **5r**, **7f**, **7j**, **7g** and **7k** exhibited maximum GI_{50}.
- Molecular docking study was also performed.
- Docking pose for the active compounds **7f**, **7g** and **7i** are shown.